OAK RIDGE NATIONAL LABORATORY
operated by
UNION CARBIDE CORPORATION
NUCLEAR DIVISION
for the
U.S. ATOMIC ENERGY COMMISSION

ORNL - TM - 2080

DESIGN OF BOILER-SUPERHEATER UNITS FOR REPRESENTATIVE CESIUM AND POTASSIUM SPACE POWER PLANTS

T. T. Robin

ORNL-TM-2080

Contract No. W-7405-eng-26

Reactor Division

DESIGN OF BOILER-SUPERHEATER UNITS FOR REPRESENTATIVE CESIUM AND POTASSIUM SPACE POWER PLANTS

T. T. Robin

SEPTEMBER 1968

OAK RIDGE NATIONAL LABORATORY
Oak Ridge, Tennessee
operated by
UNION CARBIDE CORPORATION
for the
U. S. ATOMIC ENERGY COMMISSION

Page Intentionally Left Blank

FOREWORD

This report summarizes a comparison of the effects on boiler size and weight of the use of cesium and potassium as working fluids for Rankine cycle space power plants. The work was conducted by the Oak Ridge National Laboratory for NASA under AEC Interagency Agreement 40-98-66, NASA Order W-12353. Technical management was performed by A. P. Fraas at the Oak Ridge National Laboratory, and project management for NASA was performed by S. V. Manson at NASA Headquarters.

Page Intentionally Left Blank

CONTENTS PAGE

Page Intentionally Left Blank

FIGURES

Page Intentionally Left Blank

TABLES

DESIGN OF BOILER-SUPERHEATER UNITS FOR REPRESENTATIVE CESIUM AND POTASSIUM SPACE POWER PLANTS

T. T. Robin

ABSTRACT

Boiler designs were developed for both potassium and cesium systems. Two design approaches were used. The first was based on using vortex generator inserts to centrifuge droplets to the walls and thus improve heat transfer in the transition region. The second was directed toward design for low-liquid entrainment in the boiling region. The results indicate that the cesium boiler is heavier than the potassium boiler by a factor of 1.3 for the vortex generator approach, and by a factor of 2.7 for the low-liquid entrainment approach. Further, it appears that the low-liquid entrainment approach yields boilers that are smaller by a factor of about 3 to 5 and lighter by a factor of about 2 for potassium; for cesium the weight saving from use of the low entrainment approach appears to be only about 20%.

INTRODUCTION

The Oak Ridge National Laboratory was asked by NASA to undertake a comparative study of cesium and potassium Rankine cycle systems for 300 Kw(e) space power plants with the objective of highlighting the principal differences that result from the use of one fluid or the other, and the principal advantages and disadvantages of each from the standpoint of the design and development of the individual components and the complete integrated systems (AEC Interagency Agreement 40-98-66 NASA Order W-12,353).

Design studies for a series of boilers for potassium and cesium Rankine cycle space power systems were developed. These design studies were started on the base provided by the information presented and/or referenced in companion reports, that is, thermodynamic cycle data developed in the turbine study,[1] the information gathered on potassium and cesium boilers in the survey of component and system design and test experience,[2] and the general background of experience at Oak Ridge National Laboratory in the design, operation, and control of boilers and other heat exchangers.

This report begins with a summary of the basic fluid-flow and heat-transfer considerations which affect the design of once-through boiler-superheaters. In light of these basic considerations two design

philosophies for minimizing the boiler-superheater weight and volume are outlined. Several boiler-superheater designs were developed for potassium and cesium using both of these approaches. From the resulting designs, comparisons were made between the potassium and cesium boiler-superheater units with respect to weight and volume.

The first design philosophy used was the vortex generator approach which employs a twisted tape to improve the heat transfer coefficient downstream of the point where dry-wall conditions develop. The second design philosophy used was the low-entrainment approach. Here the transition from annular flow to a dry wall condition is deferred by using a low flow rate and by reducing the temperature difference between the primary fluid and the working fluid sufficiently so that the resulting heat flux will be relatively low in the critical region.

BACKGROUND ANALYSIS

Basic Fluid-Flow and Heat-Transfer Considerations

In the design of a once-through boiler, consideration must be given to the various fluid-flow and heat-transfer regimes that prevail throughout the length of the boiler tube. These regimes may be characterized as follows:

1. Preheating with no boiling
2. Preheating with some nucleate boiling (Subcooled boiling)
3. Nucleate boiling with bubbly flow
4. Annular flow with vaporization from the surface of the film
5. Mist flow with a dry wall
6. Superheating of dry vapor.

From the design standpoint, the heat-transfer coefficient is very high throughout the first four regions so that for design purposes they can be treated as a single region with a single average heat-transfer coefficient. In the fifth region, heat transfer may occur either by the usual forced convective heat transfer through the boundary layer at the interface between the tube wall and the gas, or by impingement of liquid droplets on the wall and their evaporation. The latter,

of course, gives a much higher heat-transfer coefficient, but it is difficult to predict to what extent it will be effective, particularly since the liquid droplets tend to move in a core down the center of the channel, and will have a low probability of striking the walls unless something is done to throw them outward. In the sixth region the heat-transfer coefficient can be estimated in a straight-forward fashion from basic forced convection-heat transfer considerations.

A review of test data from once-through boilers indicates that the annular flow region fades out into a series of discrete rivulets, which rapidly dry up to give a dry-wall condition. The vapor quality at which this occurs, and hence the amount of liquid droplets entrained in the vapor stream, varies with the mass-flow rate, the Reynolds number in the vapor, the Weber number of the liquid film moving along the wall, etc., but, for the range of interest in this study, generally fell in the region of 80 to 95%. In general, the quality at which the dry wall condition occurs is reduced as the mass flow through the boiler tube is increased.

The boiler designer is, thus, confronted with a choice in his effort to minimize the boiler volume. One approach is to use a high flow rate and a high heat flux. This situation usually results in a dry-wall condition at a relatively low quality, perhaps as little as 50%. If the dry wall condition develops at, say, 80%, the heat load in the dryer-superheater will be about one-quarter that in the boiler region. Owing to the large decrease in the heat transfer coefficient from annular flow conditions to the dry wall condition, the required heat transfer surface area in the dryer-superheater becomes a significant part of the total required area, perhaps 50 to 80%. As an alternate approach, the designer may choose to use a low flow rate and a low heat flux in the high quality region of the boiler to maintain the annular flow region until the vapor quality reaches 90 to 95%. This results in a slightly longer boiling region (the increase in length is relatively small since the boiling heat transfer coefficient is large), but the resulting heat load in the dryer-superheater is much reduced, and can result in a much shorter dryer-superheater region.

Description of Design Approaches

Several different sets of conditions were used to develop a series of designs. This approach has the advantage that it shows the effects of both the design philosophy and design conditions on the relative size and weight of cesium and potassium boilers for space power systems as well as something of the advantages and disadvantages of the various designs that stem from the different conditions.

Two principal design philosophies were considered. The first used vortex generator inserts in each boiler tube. Primarily, these inserts increase the heat transfer coefficient downstream of the region in which the dry wall condition has been reached. This increase results from the centrifuging action of the vortex generator on liquid droplets dispersed in the vapor. The second design approach was aimed at minimizing the production of liquid droplets which become dispersed in the vapor. This was accomplished by keeping the vapor velocity low in the annular flow region so that droplets would not be entrained from the liquid film on the tube wall, and by deferring the transition to the dry wall condition to higher qualities. The advantage of the latter approach is that more liquid evaporation occurs from the liquid film on the tube wall, which is the more efficient place for the evaporation process. To dry out those liquid droplets that remain in the vapor, a 180° bend in the tube in the superheater region can be employed to centrifuge the dispersed droplets to the tube wall where they may be evaporated efficiently.

Vortex Generator Approach

The vortex generator has its primary effect in the transition range and produces a body force field under zero-g conditions. This effect acts to centrifuge liquid droplets to the tube wall where they evaporate and thus increases the heat transfer coefficient. Boilers employing these inserts have been designed for both parallel flow and counter-flow operation. Both AiResearch[3,4] and General Electric[5,6] have done development work on potassium boilers using this technique. Mercury boilers using vortex generators are being developed by Aerojet.[7] Aerojet has reported that their design failed to produce fully dried vapor. This means that the centrifuging action of the vortex generators is not

necessarily 100% effective (possibly in part because some liquid flows along the surface of the insert through the boiler rather than being evaporated).

Another disadvantage of the vortex generator approach is the unheated wall effect investigated by Becker.[8] This effect occurs in the annular-flow region when some liquid film covers a surface which is not heated, such as that of a twisted tape insert. Since the surface is not heated, no evaporation occurs from it. Thus, the liquid collecting on the unheated surface will not evaporate unless it can be returned to a heated surface. Further, the amount of liquid film on the heated wall tends to be significantly less than would be the case if no insert were present. Thus, the dry wall condition is reached at a lower nominal vapor quality. By forming a thermal bond between the twisted tape vortex generator and the tube wall, the tape could be made to act as a fin and reduce the above effect. However, this increases fabrication difficulties.

Low Entrainment Approach

The difficulty of evaporating liquid that has been dispersed in the vapor has led to consideration of the low entrainment approach. In this approach, an effort is made to minimize the amount of liquid which becomes entrained in the vapor.

There are several possible sources of the liquid droplets that enter the vapor core. At the transition from bubbly flow to annular flow, it is possible that some of the liquid from the ligaments between bubbles may remain dispersed in the vapor. It is not believed that this transition represents a significant source of liquid droplets, although further research to determine its magnitude would be valuable.

For water systems, bubble nucleation in the liquid film in the annular flow region has been observed by Hewitt[9] to throw liquid into the vapor core. Hewitt observed that the number of active nucleation sites was insufficient to make much contribution to the total entrainment. The question now arises: will the same phenomena occur for liquid metal systems? Considering the high thermal conductivity of the liquid metals, the temperature drop across the thin liquid film will be small even for high heat fluxes. The surface temperature will be close to the saturation

value, and thus the temperature at the liquid metal-tube wall interface will be only a few degrees higher than saturation. In light of the fact that liquid metals require large superheats for nucleation if no nucleation sites are present it appears probable that no nucleate boiling will occur in the annular flow region for these fluids, although Peterson[10] states that his results tend to indicate bubble nucleation for potassium in the annular flow region. Even if nucleation were present, the total amount of liquid entrainment that it will induce will probably be small as indicated by Hewitt. Further research may be in order to determine whether bubble nucleation in the liquid film is a significant source of liquid entrainment for liquid metals.

A third source of liquid entrainment stems from the action of the high velocity vapor on the surface of the low velocity liquid film. The film will tend to form waves and, if the vapor velocity is high enough, some liquid will be torn from the wave crests. This process has been experimentally investigated by Chien and Ibele[11] for water systems. They developed the following criterion for the transition from annular flow to annular-mist flow stemming from liquid entrainment from the wave crests:

$$Re'_g \cdot Re'^{0.301}_{\ell} = 1.199 \times 10^6 \qquad (1)$$

where

$Re'_g = 4\,\dot{m}_g/\pi D N_g$, the superficial vapor Reynolds number

$Re'_\ell = 4\,\dot{m}_\ell/\pi D N_\ell$, the superficial liquid Reynolds number

$\dot{m}_g$ = vapor mass flow rate, lb_m/sec

$\dot{m}_\ell$ = liquid mass flow rate, lb_m/sec

D = tube inside diameter, ft

N_g = vapor viscosity, $lb_m/sec\text{-}ft$

N_ℓ = liquid viscosity, $lb_m/sec\text{-}ft$

Tong[12] has reported an equation developed by Mozharov[13] for the entrainment of liquid from the liquid film. The equation predicts the

critical vapor velocity above which liquid will be entrained from waves in the liquid film and is as follows:

$$V_v^* = 115 \left(\frac{\sigma}{\rho_v} \right)^{1/2} \left(\frac{X}{D(1 - X)} \right)^{1/4} , \qquad (2)$$

where

V_v^* = the critical vapor velocity, m/sec,
σ = surface tension, kg/m,
ρ_v = vapor density, kg/m^3,
X = vapor quality,
D = tube inside diameter, m.

Equation (2) also suggests a critical mass flow rate:

$$G^* = \frac{\rho_v V_v^*}{X} . \qquad (3)$$

Equations (1) and (3) may be used to estimate mass flow rates below which no liquid entrainment from wave crests will occur.

A final possible source of liquid droplets in the vapor core is the phenomenon termed the critical heat flux. This is a complex phenomenon, and a complete understanding of it does not presently exist. At the critical heat flux condition, the heat transfer process changes from evaporation of the liquid film to that of heat convection and liquid transport through the vapor and evaporation of any liquid that impinges on the wall. The above explanation of the critical heat flux implies that something causes the liquid film to separate from the wall. There are several explanations for this occurrence. One is that the velocity of the vapor is high enough to rip the liquid off the wall. Another explanation suggests that once a dry spot appears, its surface temperature will rise. As the temperature rises, lateral conduction occurs; the local temperature and

heat flux on the rim of the dry spot increase; the area of the dry spot spreads and, eventually, the critical condition is reached.

Hewitt's study[9] of this process in water systems is significant. The following paragraph from his report is of interest:

> When a heat flux was applied, water was lost from the film by direct evaporation from the liquid surface or by generation of steam bubbles on the heated rod (i.e., by nucleation). The reduction of the water flow rate in the film led to the attenuation of the large disturbance waves on the film surface and eventually, at a point near the top of the heater, a small dry patch began to appear intermittently. This dry patch began to grow down the rod and others appeared around it as the heat flux was further increased. The liquid flowed in narrow streams around the dry patches which now had a continuous existence, although their boundaries were oscillating. The areas of the surface which were dry were, of course, still being heated and the rod rose in temperature at these points; eventually this rise in temperature was sufficient to cause the resistance-operated trip to come into action.

Hewitt concluded that the "dry-wall" phenomenon was clearly the result simply of progressive loss of water from the film by evaporation and entrainment, and the local value of the heat flux at the site of the transition was of only secondary relevance.

Hewitt's conclusion that the heat flux is of only secondary relevance should be qualified if a wide variety of conditions is to be considered. For an overall indication of the characteristics of the critical heat flux condition from 0 to 100% quality, it has been useful to consider the critical heat flux as a function of the critical quality. This correlation suggests that the critical heat flux decreases as the quality increases. (For potassium, experimental data are plotted in this manner in Fig. 9, p. 28, which was produced by Bond and Converse.[6]) The designer should keep the heat flux below the indicated critical value if he wishes to avoid a dry wall condition from the inlet up to the desired high quality region.

In the high quality region, the heat flux becomes less important (as indicated by Hewitt), and the mass flow rate has a strong effect on the transition from annular flow to the dry wall condition. In general, the higher the mass flow rate the lower the critical quality. For the

case of potassium, Yarosh[14] has concluded that the same relation holds. Thus, to defer the transition from annular flow to the dry wall condition, the designer should provide a low flow rate near the high quality end.

Another possible source of liquid droplets might be associated with the wetting characteristics of the working fluid. Experience with mercury has shown that it does not wet steel well, and hence it gives an unstable annular-flow region. However, since potassium is known to be strongly wetting, poor wetting was not considered as a factor in this work.

Four possible sources have been cited for liquid droplets in the vapor core:

1. Transition from bubbly flow to annular flow.
2. Nucleation and bubble release from the liquid film in the annular flow region.
3. Entrainment of liquid from wave crests in the annular film.
4. Transition to the dry-wall condition.

The low entrainment approach to the design of once-through boiling operation has the objective of minimizing the above sources. The first source appears unavoidable, but it is not believed to be large, and, if some liquid droplets are formed at this point, they have almost the entire length of the boiler tube to re-enter the liquid film. The second source is not believed to be a factor for alkali metal systems. The third source may be eliminated by keeping the vapor velocity low enough so that the criterion of Eq. (1) or Eq. (3) is satisfied.

To minimize the effect of the fourth source an effort can be made to prolong the annular flow region, that is, to increase the value of both the critical heat flux and the critical quality at which it occurs. Several measures appear possible in this case. First, assuming that the critical heat flux is not exceeded in the low quality region, the vapor velocity may be made small enough so that it will not tend to generate large waves in the liquid film and thus help to avoid a transition from annular flow to a dry wall condition caused by high vapor velocity. Secondly, textured surfaces may be used which will help keep the liquid film on the wall. Finally, the heat flux at the high quality end of the boiler may be kept below the value which characterizes the transition

from annular flow to the dry wall condition. After the geometry and flow rates are fixed, the heat flux is controlled by the temperature difference between the primary fluid and the working fluid. A low heat flux in the high quality region of the boiler can be obtained by using a parallel-flow arrangement rather than a counterflow arrangement which would give the maximum heat flux in the high quality region.

Unfortunately, the high quality end adjoins the superheater region. Low heat fluxes in this region result in an unacceptably large surface area requirement for the superheater. A more appropriate arrangement would be to have a parallel-flow boiler up to the dry wall region and then have a counterflow arrangement for the dryer-superheater. This arrangement can be obtained if the primary fluid enters both ends of the boiler and exits from the boiler in the vicinity of the "critical heat flux" region. As shown in Fig. 1, this arrangement requires an extra entrance for the primary fluid as compared to the more conventional arrangement. The flow rates of the primary fluid entering the two regions may be orificed so that the change in fluid temperature of the two streams will be the same. This orificing would result in a low temperature difference in the high quality region of the boiler while still giving a relatively large temperature difference for the superheating process. An improvement over this orificing is illustrated in Fig. 2. In this case, the flow fraction through the boiler is made smaller than for the case of Fig. 1. The temperature difference at the exit of the boiling region can thus be adjusted to as low a value as desired, and the heat flux at the exit of the boiling section can be made low enough to defer the dry wall condition until a high vapor quality is obtained. Also, since the primary fluid flow rate in the parallel portion is reduced, that in the counterflow (dryer-superheater) region must be increased. This adjustment increases the overall temperature difference in the dryer-superheater and results in a reduction in the required heat transfer area. The only apparent penalty is the practical problem of mixing two liquid metal streams having a substantial temperature difference.

ORNL DWG. 68-8587

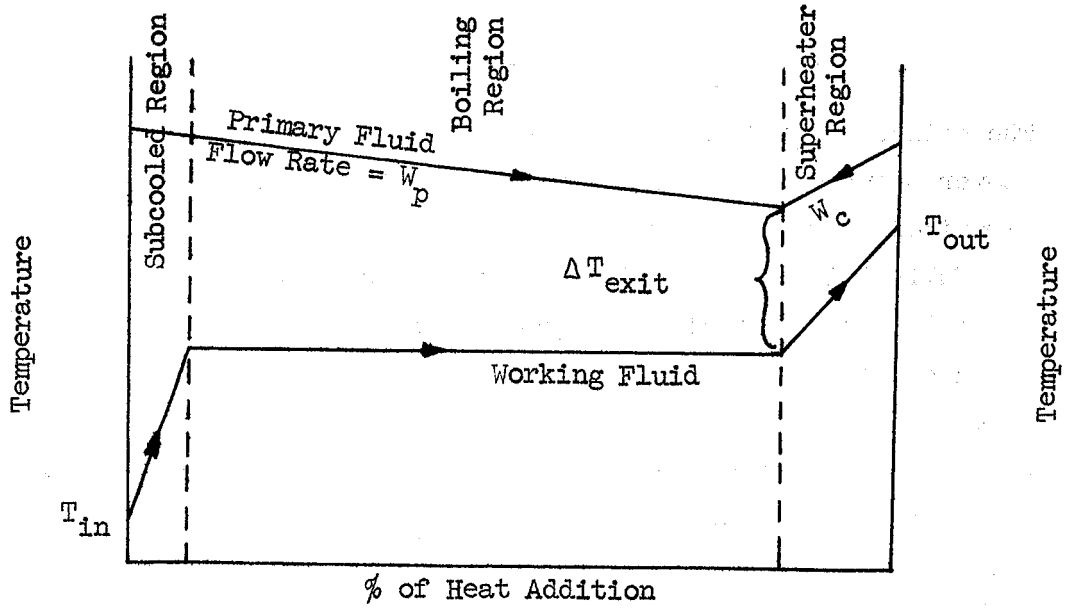

Fig. 1. Parallel-Flow Boiler and Counterflow Superheater with Orificing for Equal Primary Fluid Temperature Drops in Both Regions.

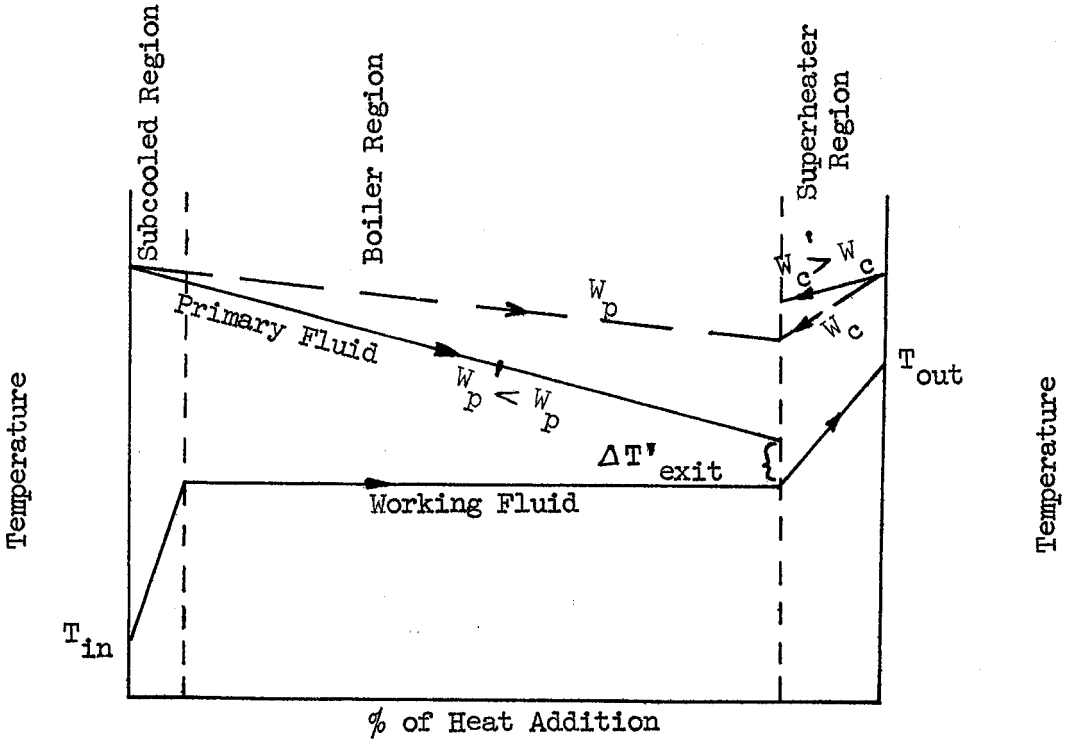

Fig. 2. Parallel-Flow Boiler and Counterflow Superheater with Adjusted Orificing.

DESIGN

General Boiler Requirements and Design Precepts

The boilers considered in this study are components in complete space power plant systems. The requirements these boilers must satisfy are summarized in Table 1. Note that the vapor at the exit of the boiler is to be fully dried (no liquid droplets) and superheated.

The boiler design work was approached by dividing the boiler into three regions: The preheater region, the boiler region, and the superheater region.* The first task was to estimate the heat loads in each region. This requires an assumption about the operating pressure in the boiling region. For both cesium and potassium the pressure in the boiling region was assumed constant and equal to the pressure at the exit of the boiler. If the pressure drops are small, this assumption will be approximately true. If the pressure drops are large, the calculated design values will need some adjustment for a final design. However, for the purpose of this comparison between cesium and potassium, the above assumption was found to be acceptable.

After estimating the heat loads, the temperature difference at the entrance and exit of each section was calculated. With these values, the LMTD was calculated for each region. Based on the assumed geometry, the overall heat transfer coefficient, U, was calculated. The required heat transfer area for each region was then estimated:

$$\text{Area} = \frac{\text{Heat Load}}{\text{LMDT x U}} \tag{4}$$

From the area, the length of tubing required was calculated together with the pressure drop across the boiler.

---

*For the low entrainment designs, the subcooled and boiling regions were further divided; however, these calculations were done on a computer program which will be discussed in a later section.

Table 1. Boiler Requirements

	Exit Temperature (°F)	Exit Pressure (psia)	Flow Rate (lb/sec)	Total Energy Load (Btu/lb)	Primary Fluid (Li) Inlet Temperature (°F)	Primary Fluid (Li) Exit Temperature (°F)
Potassium Boiler	2150	214.3	2.22	752.1	2300	2200
Cesium Boiler	2150	314.6	8.9	187.0	2300	2200

Vortex Generator Design

The equations and procedures used for developing the boiler heat transfer coefficient were developed by Peterson.[5] The procedure was referred to as the average parameter approach. The equations and symbols used for this approach are summarized in Appendix A.

The major design information for this approach is shown in a curve of average heat transfer coefficient from 0 to 100% quality versus the radial acceleration (See Fig. 3 and Appendix A). For radial accelerations between 80 and 100 g's, the average boiling heat transfer coefficient varies from about 3500 to 6000 Btu/hr-ft^2-°F. This information was developed from experimental data for potassium. Similar data were not available for cesium. A widely accepted procedure for estimating the heat transfer characteristics of boiling cesium from the data for boiling potassium was not available. For lack of anything more appropriate Fig. 3 was also used for the cesium.

In order to reduce the area required for the boiling section, a high value of the average boiling heat transfer coefficient is required. This, in turn, requires a high radial acceleration. To produce a high radial acceleration, the number of boiler tubes should be kept low, yet pressure drop considerations require a relatively large number of tubes for the cesium design. Another requirement was that the average boiler heat flux be kept below 200,000 Btu/hr-ft^2 which represents the upper limit of the

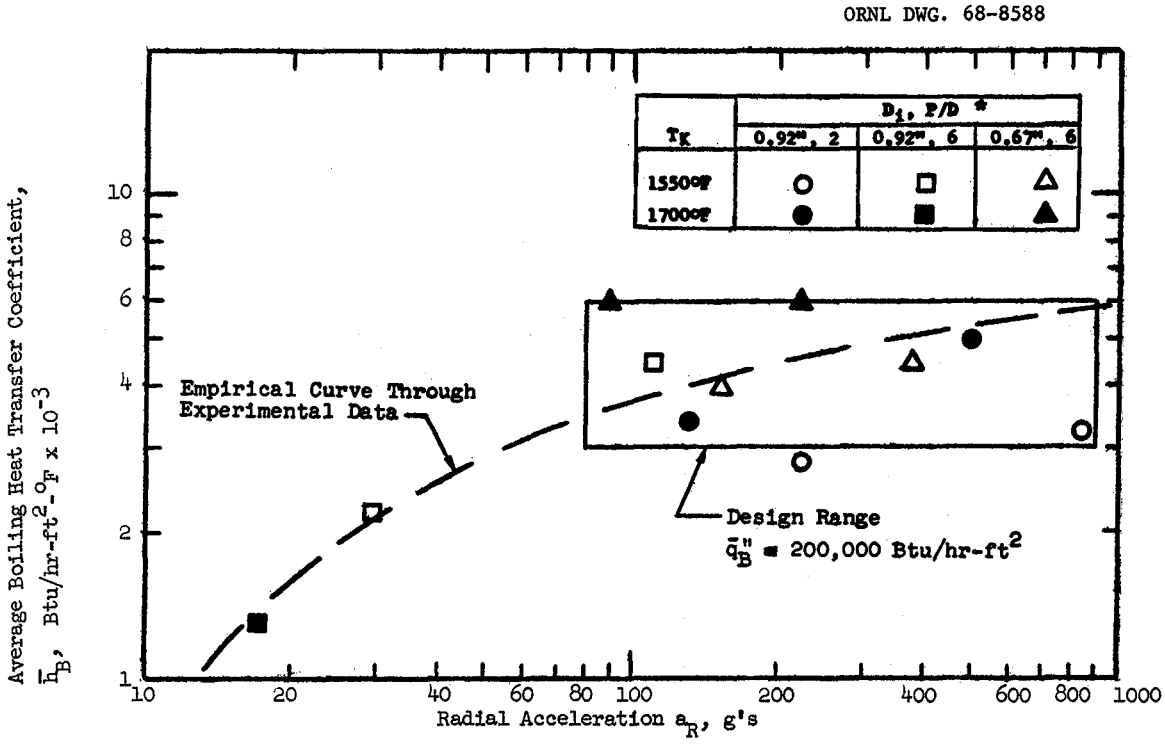

Fig. 3. Curve of Average Heat Transfer Coefficient from 0 to 100% Quality vs the Radial Acceleration. (Peterson, Ref. 5)

experimental data (see Fig. 3). This number is directly proportional to the overall heat transfer coefficient and LMTD. The overall heat-transfer coefficient is in part dependent on the tube spacing, and this was adjusted so that the above average heat flux was not exceeded.

The design precepts used for these boilers are listed in Table 2. Table 3 gives the step-by-step calculation procedure for the boiler design.

Table 2. Design Precepts for the Vortex Generator Approach

1.	Tube ID of 0.75 in.
2.	Tube wall thickness of 0.03 in.
3.	Vortex generator insert constructed of a solid rod with a metal ribbon wrapped spirally around it to give a spiral pitch-to-tube diameter ratio of 1.0 with a ratio of the solid rod OD to the tube ID of 0.2 (this construction is similar to that of Ref. 15.)
4.	The conductivity of the tube wall material equals 35 Btu/hr-ft-°F.
5.	The average heat transfer coefficient in the boiling region was taken from Fig. 3.
6.	The average heat flux in the boiling region should be kept less than 200,000 Btu/hr-ft^2 by adjusting the tube spacing.
7.	Counterflow.
8.	Equilateral triangular tube array.

Table 3. Details of Vortex Generator Design Procedure

Line Number	Item	Source	Cesium	Potassium
1	Average pressure in boiler, psi	Assumed	314.6	214.3
2	Average saturation temperature in boiler, °F	NRL-6246, NRL-6233 (Ref. 25, 26)	2125	2125
3	Vapor enthalpy, Btu/lb	NRL-6246, NRL-6233	316.66	1223.47
4	H_{fg}, Btu/lb	NRL-6246, NRL-6233	167.83	718.55
5	Liquid enthalpy, Btu/lb	NRL-6246, NRL-6233	148.83	504.92
6	Quality at exit of boiling region, %	Assumed	100	100
7	Enthalpy at exit of boiling region, Btu/lb	(3)	316.66	1223.47
8	Primary fluid inlet temperature, °F	Assumed	2300	2300
9	Primary fluid outlet temperature, °F	Assumed	2200	2200
10	Temperature of working fluid at exit, °F	Given	2150	2150
11	Pressure of working fluid at exit, psia	Given	314.6	214.3
12	Enthalpy of working fluid at exit, Btu/lb	Given	320	1230.5
13	Flow rate of working fluid, lb/sec	Given	8.9	2.22
14	Total heat load, Btu/lb	Given	187.0	752.1
15	Heat load in superheater, Btu/lb	(12) − (3)	3.34	7.03
16	Heat load in boiling region, Btu/lb	(4)	167.83	718.55
17	Heat load in subcooled region, Btu/lb	(14) − (15) − (16)	15.83	26.52
18	Flow rate of primary fluid, lb/sec	(14) x (13)/c_p x ((8) − (9))	16.97	17.01
19	Number of boiler tubes	Assumed	45	19
20	Tube-wall thickness, in.	Assumed	0.03	0.03
21	Tube ID, in.	Assumed	0.75	0.75
22	Diameter to pitch ratio for vortex generator	Assumed	1.0	1.0
23	Ratio of vortex generator support rod diameter to tube ID	Assumed	0.2	0.2
24	Equivalent diameter in tube, in.	$(21) \times \left[\frac{1-(23)^2}{1+(23)+\frac{1}{\pi}(1-(23))}\right]$	0.494	0.494
25	Flow area per tube, ft^2	$(\pi/4)\left[(21)^2-(21)\times(4)^2\right]\frac{1}{144}$	0.00295	0.00295

Table 3. (continued)

Line Number	Item	Source	Cesium	Potassium
26	Tube spacing, in.	Assumed	0.4	0.8
27	Tube OD, in.	(20) + (21) x 2	0.81	0.81
28	Center-to-center tube spacing, in.	(27) + (26)	1.21	1.61
29	Equivalent diameter on shell side, in.	$(27) \times \left[1.102 \left((28)/(27)\right)^2 - 1\right]$	1.176	2.72
30	Flow area on shell side, ft^2	$2 \times \frac{(19)}{144} \left[0.433 \left((28)\right)^2 - 0.39 \left((27)\right)^2\right]$	0.236	0.207
31	Radial acceleration, g	See Appendix A, Eq. (A2)	184	730
32	Average heat transfer coefficient in boiling region, Btu/hr-ft^2-°F	See Fig. 3	4000	6000
33	G c_p for primary fluid, Btu/sec-ft^2-°F	(18) x c_p/(30)	70.8	80.5
34	k/D for primary fluid, Btu/hr-ft-°F-in.	k/(29)	25.5	10.85
35	Heat transfer coefficient on primary side, Btu/hr-ft^2-°F	(34), (33), Fig. H5.15 of Ref. 16	3800	2300
36	G c_p for working fluid in subcooled region, Btu/sec-ft^2-°F	(13) x c_p/(25) x (19)	2.89	6.30
37	k/D for working fluid in subcooled region, Btu/hr-ft-°F-in.	k/(24)	13.06	27.5
38	Heat transfer coefficient in subcooled region (neglecting radial acceleration), Btu/hr-ft^2-°F	(37), (36), Fig. H5.15 of Ref. 16	1000	1500
39	Heat transfer coefficient in superheater, Btu/hr-ft^2-°F	See Appendix A, Eq. (A1)	71	108
40	Primary fluid temperature at inlet of subcooled region, °F	(9) + (15) x (13)/(18) x c_p	2208.34	2203.5
41	Primary fluid temperature at inlet of boiling region, °F	(8) - (17) x (13)/(18) x c_p	2298	2299
42	Working fluid temperature at inlet to subcooled region, °F	(2) - (17)/c_p	1850	2005
43	Temperature difference at inlet to subcooled region, °F	(8) - (42)	350	195
44	Temperature difference at inlet to boiling region, °F	(40) - (2)	73.4	78.5
45	Temperature difference at inlet to superheater, °F	(41) - (2)	173	174

Table 3. (continued)

Line Number	Item	Source	Cesium	Potassium
46	Temperature difference at exit of superheater, °F	(8) − (10)	150	150
47	LMTD in subcooled region, °F	Fig. H4.1 of Ref. 16	175	130
48	LMTD in boiling region, °F	Fig. H4.1 of Ref. 16	115	125
49	LMTD in superheater, °F	((46) + (45))/2	161	162
50	Thermal conductivity of tube wall material, Btu/hr-ft-°F	Assumed	35	35
51	Tube wall thickness, in.	Assumed	0.03	0.03
52	Overall heat transfer coefficient in subcooled region, Btu/hr-ft^2-°F	$[1/(38) + (51)/(50) \times 12 + 1/(35)]^{-1}$	744	850
53	Overall heat transfer coefficient in boiling region, Btu/hr-ft^2-°F	$[1/(32) + (51)/(50) \times 12 + 1/(35)]^{-1}$	1710	1490
54	Overall heat transfer coefficient in boiling region, Btu/hr-ft^2-°F	$[1/(39) + (51)/(50) \times 12 + 1/(35)]^{-1}$	69.0	102.5
55	Required area in subcooled region, ft^2	(17) x (13) x 3600/(47) x (52)	3.86	1.955
56	Required area in boiling region, ft^2	(16) x (13) x 3600/(48) x (53)	27.3	30.8
57	Required area in superheater, ft^2	(15) x (13) x 3600/(49) x (54)	9.8	3.385
58	Heat transfer area per foot of boiler, ft^2/ft	(19) x π x ((21) + (20))/12	9.11	3.85
59	Length of subcooled region, ft	(55) / (58)	0.424	0.508
60	Length of boiling region, ft	(56) / (58)	3.00	8.0
61	Length of superheater	(57) / (58)	1.075	0.87
62	L/L_H	$(1 + [\pi \times (23)]^2)^{1/2}$	3.3	3.3
63	Reynolds number of liquid times L/L_H	(24) x G/μ_ℓ x (62)	1.2×10^5	6.74×10^4
64	Reynolds number of vapor times L/L_H	(24) x G/μ_v x (62)	5.01×10^5	3.50×10^5
65	Liquid friction factor	$0.316/((63))^{1/4}$	0.0166	0.020
66	Vapor friction factor	$0.316/((64))^{1/4}$	0.01275	0.01396
67	Two phase pressure drop multiplier*	Ref. 17	170	65

*The combination of physical properties that determines the two-phase pressure drop has the same value for cesium at 2125°F as for potassium at 1750°F.

Table 3. (continued)

Line Number	Item	Source	Cesium	Potassium
68	Pressure drop in boiling region, psi	(60) x ((65)/(24)) x $G^2/2\rho_f g_c$ x ((62))^3 x (67)	51.2	44.0
69	Pressure drop in superheater	(61) x ((66)/(24)) x $G^2/2\rho_v g_c$ x ((62))^3 x (67)	1.72	2.96
70	Momentum pressure drop	Fig. H 3.3 of Ref. 16	0.27	0.33
71	Density to structural material, gm/cm^3	Assumed	8.9	8.9
72	Center to center tube spacing, in.	(28)	1.21	1.61
73	Shell inside radius, in.	Fig. H 6.3 of Ref. 16 (72)	4.84	4.025
74	Pressure on primary side, psi	Assumed	50	50
75	Pressure on vapor side, psi	Assumed	350	250
76	Design pressure difference for header sheets, psi	(75) − (74)	300	200
77	$S_{max}\ t^2/P$ x r^2 for header sheet	Fig. H 8.2 of Ref. 16, (72)	3.3	2.6
78	Header sheet thickness, in.	(76) × (73) × $\sqrt{2(77)}$ /2 S_{max} Sin 45°	1.08	0.64
79	Volume of holes in header sheet, ft^3	(19) x π x ((27))^2 x (78)/4 x 1728	0.145	0.0362
80	Metal volume in header sheet, ft^3	$[\pi(\frac{\pi}{2}(73)/\text{Sin } 45°)^2 \times (78)/1728] -$ (79)	0.375	0.195
81	Weight of header sheet, lb	(71) x 62.4 x (80)	20.7	10.8
82	Header thickness, in.	(75) x (73)/2 x S_{max}	0.434	0.258
83	Header weight, lb	2 π ((73))^2 (82) x (71) x 62.4/1728	20.5	8.44
84	Shell thickness, in.	(74) x (73)/S_{max}	0.124	0.103
85	Shell weight, lb	2 π (73) x (84) x ((60) + (61) + (59) + 2 x (78)) x (71) x 62.4/1728	73.9	97.9
86	Equivalent tube thickness, in.	((21) x (23))^2/(20) + (21)	0.03745	0.03745
87	Weight of tubes, lb	(71) x (86) x ((56) + (57) + (55)) x 62.4/12	67.6	63
88.	Total dry weight, lb	2 × (81) + 2 × (83) + (85)	224.3	199.4
89.	Total wet weight, lb	(88) + Lithium volume × ρ_{Li} + $\frac{2}{3}\pi$ ((73))^3 $\rho^{\ell}_{\text{working fluid}}$	282.3	278

Low Entrainment Design

The precepts for the approach to the low entrainment design are listed in Table 4. The first requirement in these design calculations was to determine the maximum flow per tube so that entrainment of liquid from wave crests will not occur. For this purpose, the Chien and Ibele criterion expressed in Eq. (1) was used. The results are given in Figs. 4 and 5 for several values of the mass flow rate for potassium and cesium in straight tubes. The data correlated by Eq. (1) show some scatter as might be expected. Thus, the value used for the mass flow rate should be chosen to be conservative to some degree. From Figs. 4 and 5, it appears that a mass velocity of about 40.0 $lb_m/sec \cdot ft^2$ will be acceptable for axial flow through a straight tube.

The Chien and Ibele criterion suggests that it would be advantageous to taper the tubes so that the vapor velocity will be roughly constant throughout the length of the boiling region. Inasmuch as the surface-volume ratio increases as the tube diameter is reduced, this approach will help reduce the boiler volume and weight. Further, while the problem is too complex to treat here, tapering the tubes has a beneficial effect on boiling flow stability by increasing the pressure drop per unit of length in the first portion of the boiler and reducing it in the latter portion. Although the use of tapered tubes is unorthodox, and might appear to present a procurement problem, developments in tube reducing in recent years have made high quality tapered tubes production items that are available from a number of well-established vendors.

Curves similar to those in Figs. 4 and 5 were prepared for tapered tubes and are shown in Figs. 6 and 7. These curves required an assumption concerning the tube ID as a function of quality. This relation was assumed to be a linear function with an ID of 0.2 in. at 0% quality, and a value of 0.45 in. at 100% quality. A linear relation does not give an exactly constant vapor velocity in a uniformly tapered tube; however, the results will give a reasonably good estimate of the effect of the tapered tube. A mass flow rate of 0.03865 lb_m/sec (which is equivalent to 35 $lb_m/sec \cdot ft^2$ at the end of the tapered section) appears to be a reasonable value for an acceptable flow rate.

Table 4. Design Precepts for the Low Entrainment Approach

1. Tube wall thickness of 0.03 in.
2. Tube ID of 0.45 in. for straight tube boilers. For tapered tube boilers, the inlet ID was taken as 0.20 in. and the exit ID 0.45 in. The tapering would end at the exit of the boiling region, and the tube would be straight with an ID of 0.45 in. through the superheater.
3. Equilateral triangular tube array.
4. Parallel-flow in the boiling region and counterflow in the superheater section with orificing of the primary fluid stream to produce a low temperature difference at the exit of the boiling region.
5. The conductivity of the tube wall material was assumed to be 35 Btu/hr-ft-°F.
6. A boiling heat transfer coefficient of 10,000 $Btu/hr\text{-}ft^2\text{-}°F$ was assumed for both potassium and cesium.
7. The mass flow rate per tube and the heat flux were kept low enough so that the flow would be in the annular region up to the specified vapor quality.
8. Simple axial fins inside the superheater tubes would serve to triple the surface area over a bare tube of the same ID.
9. The superheater area requirements were based on the heat transfer coefficient of pure vapor.
10. The spacing between tubes was held constant at 0.0625 in.

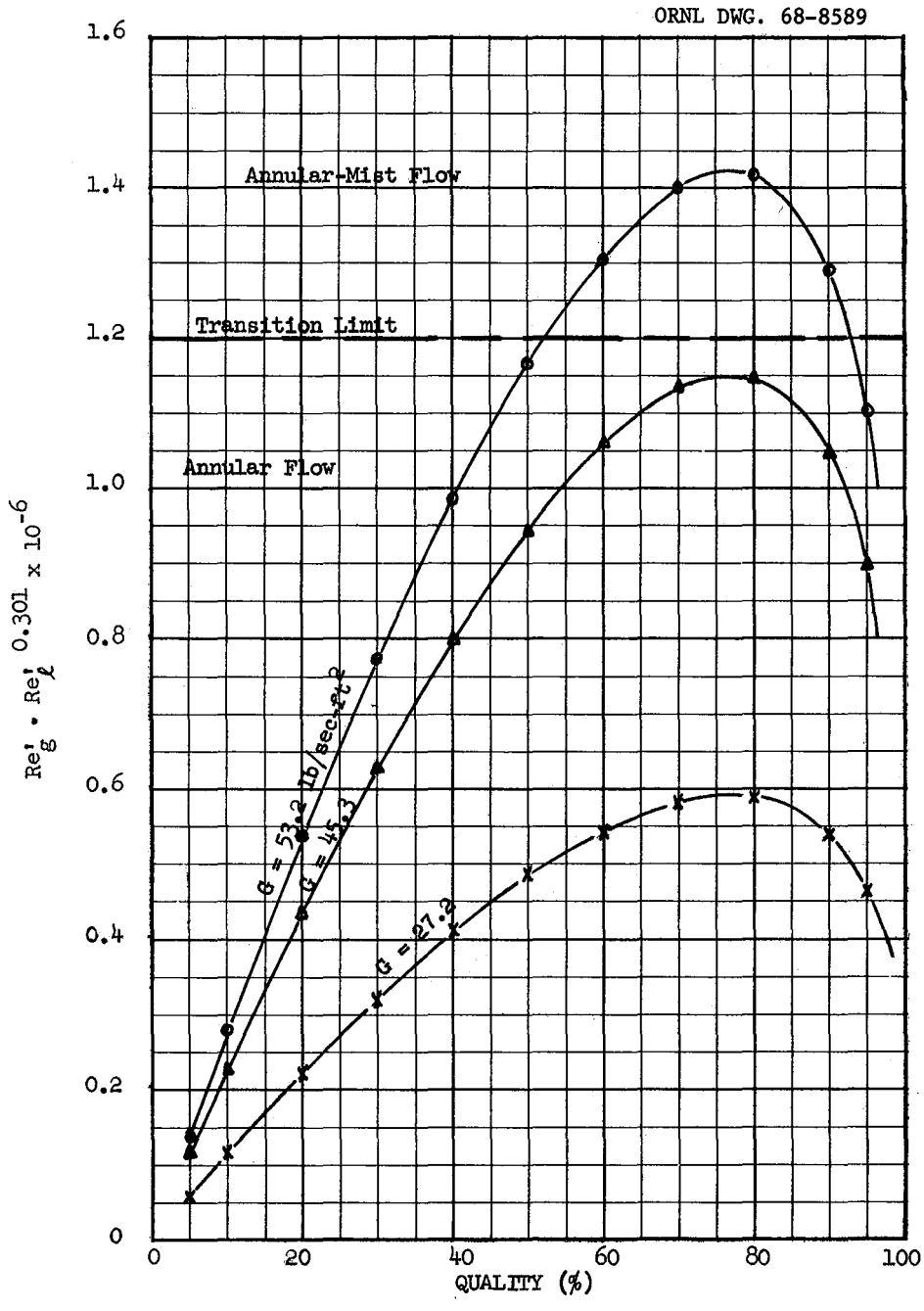

Fig. 4. Chien and Ibele Correlation of the Transition from Annular Flow to Annular-Mist Flow for Potassium in Straight Tubes.

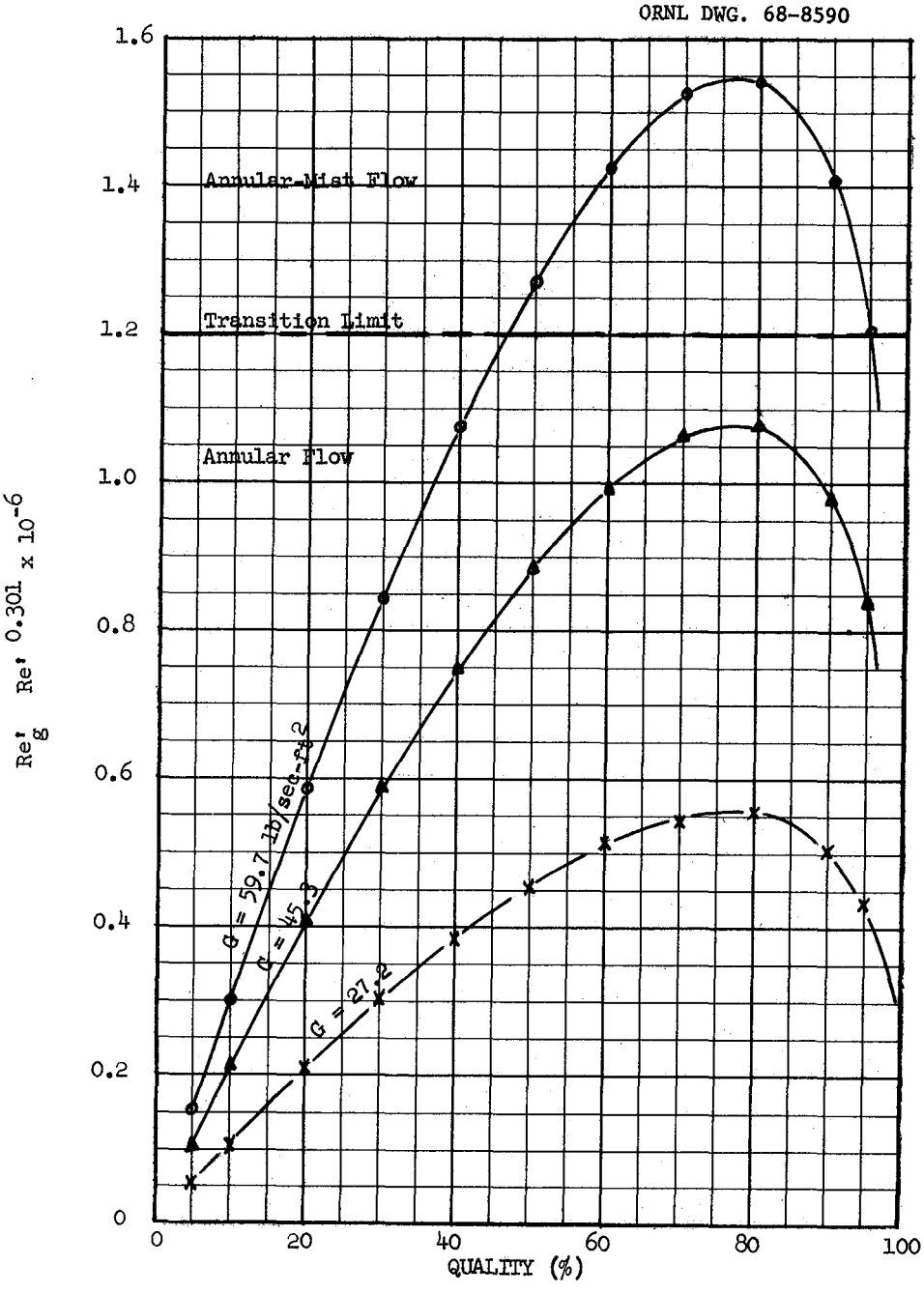

Fig. 5. Chien and Ibele Correlation of the Transition from Annular Flow to Annular-Mist Flow for Cesium in Straight Tubes.

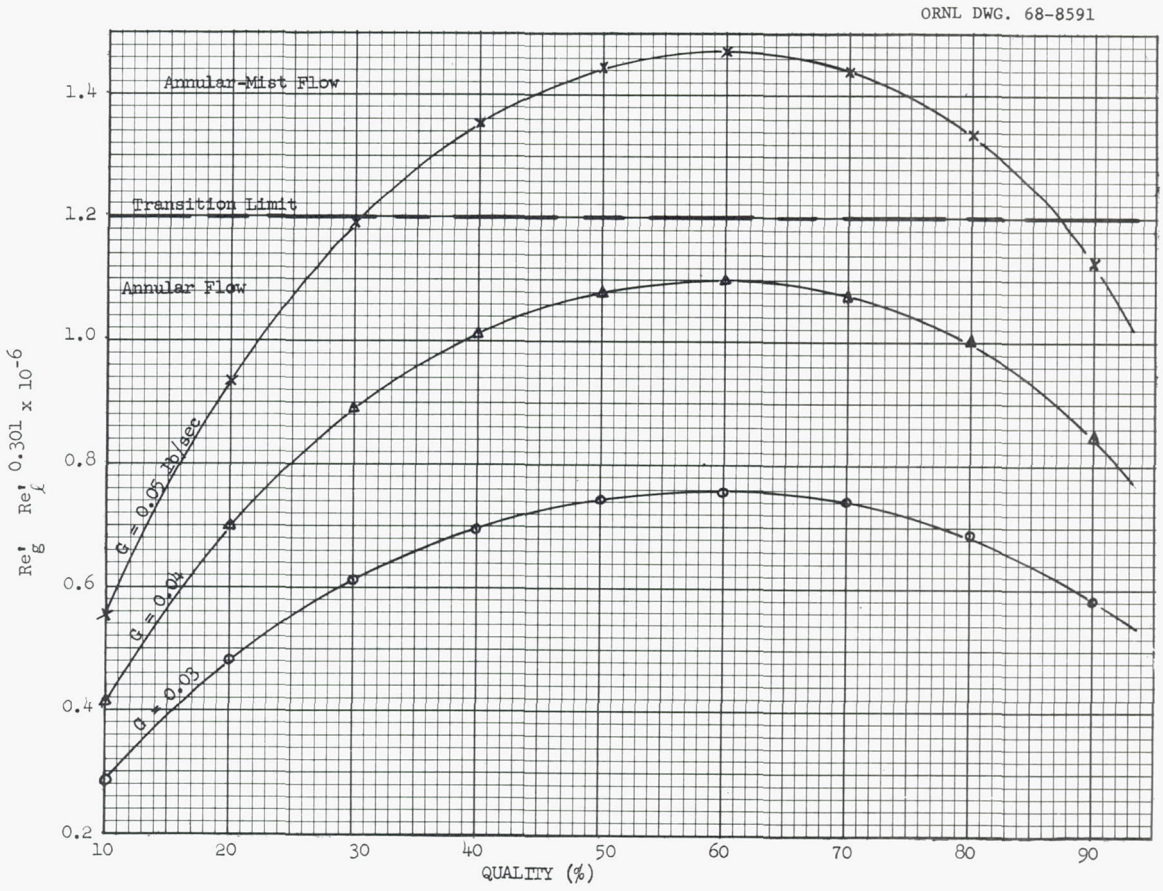

Fig. 6. Chien and Ibele Correlation of the Transition from Annular Flow to Annular-Mist Flow for Potassium in Tapered Tubes.

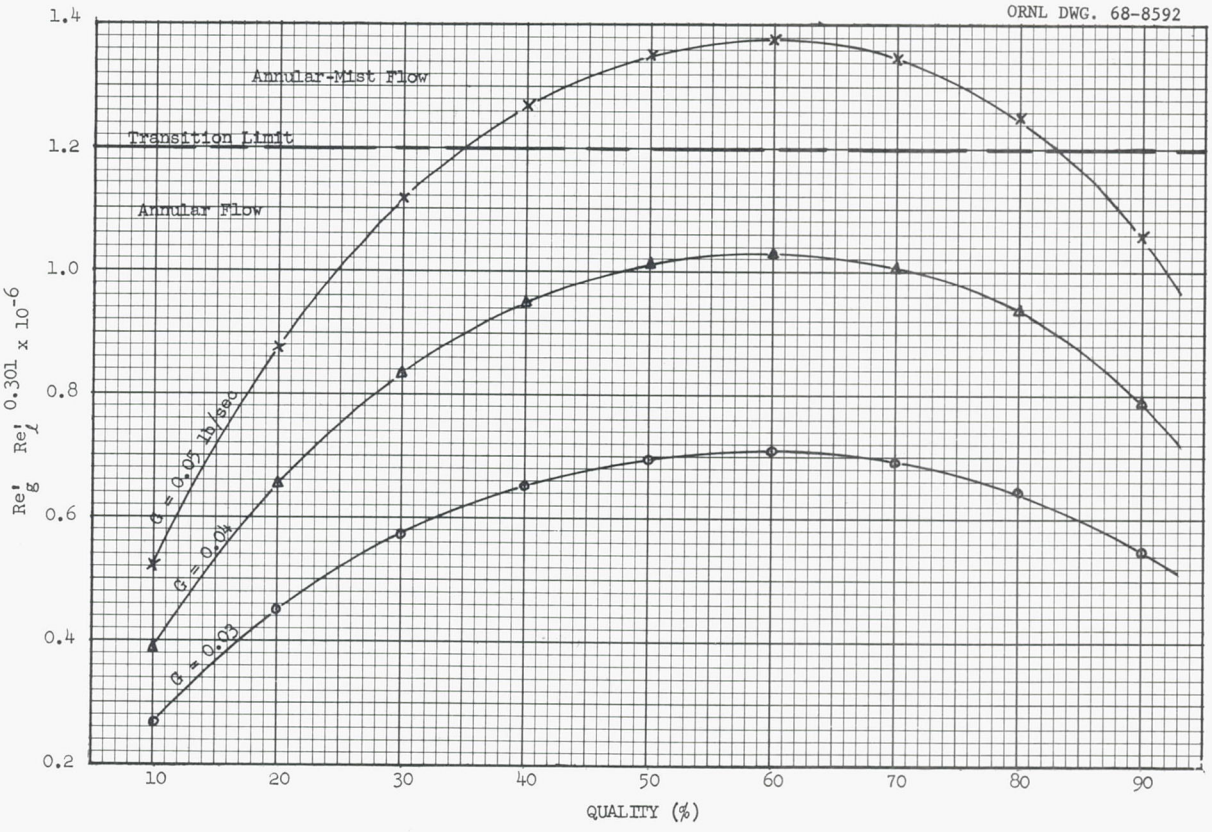

Fig. 7. Chien and Ibele Correlation of the Transition from Annular Flow to Annular-Mist Flow for Cesium in Tapered Tubes.

Mozharov's criterion (Eqs. 2 and 3) for the entrainment of droplets from the liquid film was also used to estimate the maximum allowable mass velocity for the straight tube designs. The results are given in Fig. 8. For potassium, the maximum mass velocity is predicted to be about 20 $lb_m/sec\text{-}ft^2$ which is about 50% lower than the Chien and Ibele prediction. ORNL experience indicates that the data on which Mozharov's criterion[13] was based were low as a consequence of poor wetting. Thus the Chien and Ibele criterion was used for the present study. An additional straight tube design for potassium was developed using a mass velocity of 20 $lb_m/sec\text{-}ft^2$ to indicate the magnitude of the trend if Mozharov's criterion were more nearly correct.

The second relation to be established for these designs is that between the quality and the heat flux at the critical condition. The phenomena are complex, and only rough estimates may be made at this point. For the case of potassium, the data reported by Bond and Converse[18] is useful. These data are reproduced in Fig. 9 and Table 5. For a 0.43-in.-ID tube with a flow rate of about 47 $lb_m/sec\text{-}ft^2$, the critical condition was a heat flux of about 50,000 $Btu/hr\text{-}ft^2$ at a quality of 90%. From these values and the correlation represented by Fig. 9, the following values were selected as design limits:

Quality (%)	Heat Flux ($Btu/hr\text{-}ft^2$)
86.5	65,000
90.0	50,000
93.5	35,000
97.0	20,000

The above values are in line with experimental investigations performed at ORNL[19] for potassium. The boilers were designed to give the critical heat flux condition for the specified quality at the exit of the boiler region. Each of the above listed conditions was selected for a separate design.

For cesium, almost no critical heat flux data exist. As in the vortex generator designs, for the present study, the simplest and most

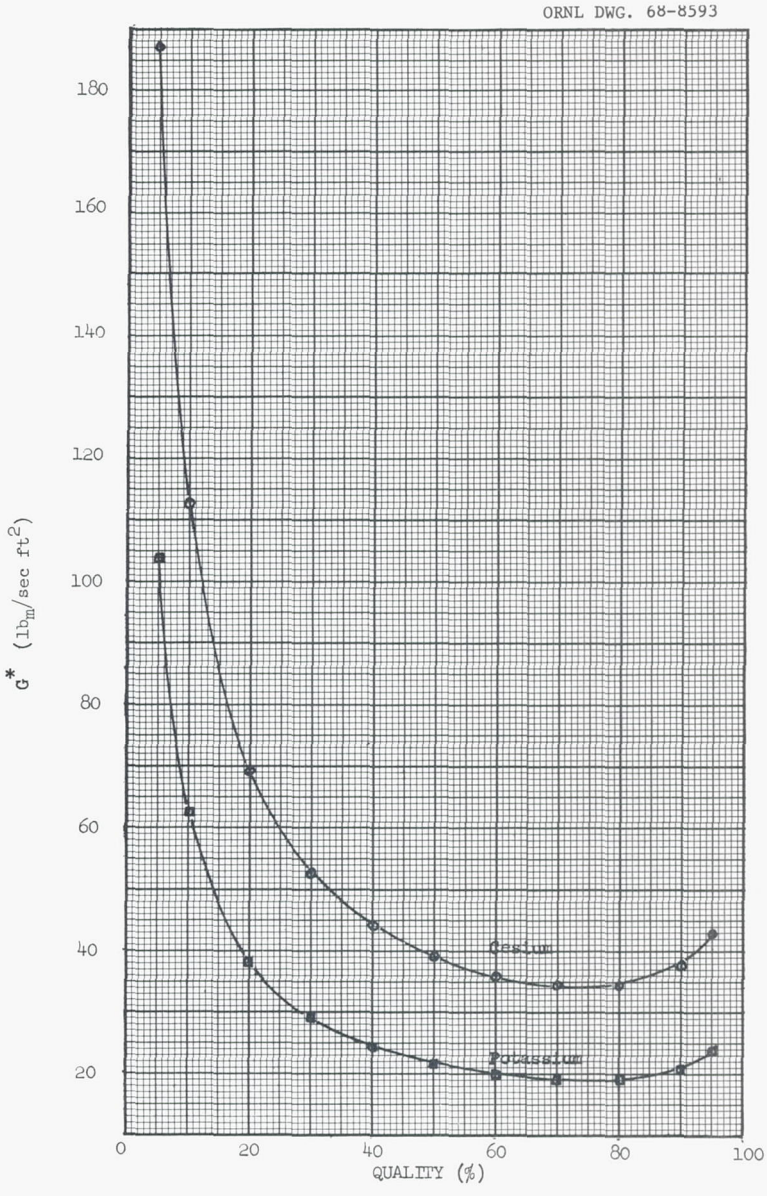

Fig. 8. Mozharov's Criterion for Entrainment of Droplets.

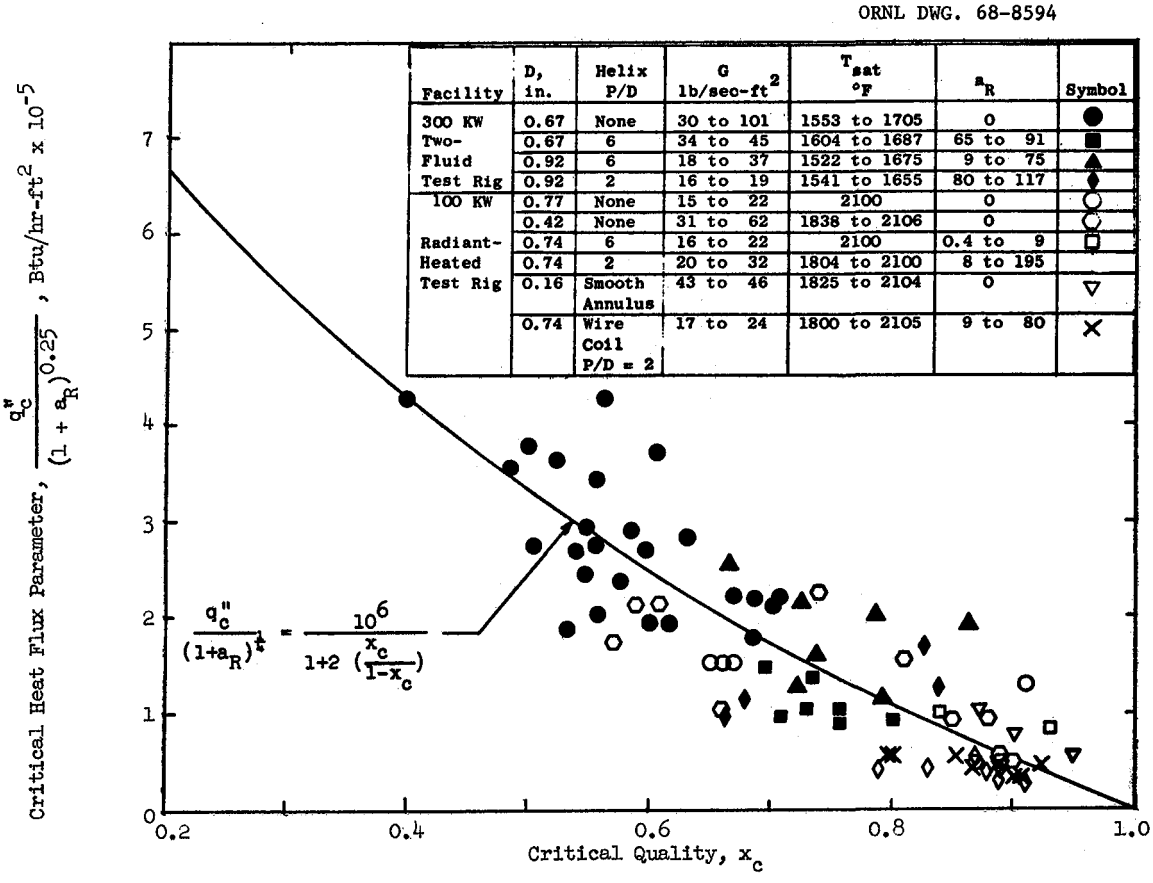

Fig. 9. Potassium Critical Heat Flux Data and Empirical Correlation. (Bond, Ref. 6)

Table 5. Potassium Critical Heat Flux Data for a 0.45-in. ID Tube (Data taken from Ref. 6)

Saturation Temperature (°F)	Flow Rate ($lb_m/sec\text{-}ft^2$)	Critical Quality (%)	Critical Heat Flux ($Btu/hr\text{-}ft^2$)
2105	61.6	81	157,000
2102	61.7	74	224,000
2100	31.0	66	101,000
1838	41.2	57	171,000
2104	47.6	88	95,000
2104	47.6	85	94,000
2105	47.6	89	50,000
2105	47.6	90	50,000
2105	47.6	89	53,000
2105	47.6	87	50,000
2105	46.7	59	211,000
2106	46.5	61	214,000

reasonable procedure was to assume that these characteristics for cesium are the same as those for potassium.

In an effort to minimize the system weight, one would like to use a small spacing between boiler tubes. This has several effects. First, the resulting boiler shell inside diameter is smaller, and thus the thickness of the casing and the surface area are smaller. This results in smaller casing weight. Second, the primary fluid inventory is reduced and this also results in a smaller expansion tank. Using tapered tubes gives the boiler a larger heat transfer surface area per unit volume and the primary liquid inventory is further reduced. Also, tapered tubes probably result in more stable two-phase flow operation than straight tubes. Additional information concerning flow stability is given in Ref. 20. Orifices may be placed near the tube inlet to

increase flow stability and provide nucleation sites. The parallel-flow arrangement will result in high temperature differences between the primary fluid and the working fluid at the inlet end which will also enhance nucleation. The high superheat requirement to initiate boiling in liquid metals is discussed in Ref. 21.

After selecting the working fluid flow rate per tube, the quality and heat flux at the exit of the boiling region and the geometry, the next quantity to be selected was the primary fluid flow rate in the boiler region. This value was primarily determined by the allowable heat flux at the exit of the boiler region. This heat flux is equal to the product of the overall heat transfer coefficient and the temperature difference between the primary fluid and the working fluid. For the geometries selected, the overall heat transfer coefficient was approximately 4000 Btu/hr-ft^2-°F. For the case of 90% quality at the boiler exit, the heat flux limit was 50,000 Btu/hr-ft^2, and thus the required temperature difference at the exit of the boiler region is approximately

$$\frac{50,000}{4,000} = 12.5°F \quad .$$

The temperature of the working fluid was set by the pressure, and was approximately 2125°F; thus the primary fluid exit temperature was about 2138°F. Since the heat load (Btu/sec) in the subcooled region and the boiling region are known, along with the primary fluid inlet temperature (2300°F), the primary flow rate may be calculated from $Q = \dot{m}C_p\Delta T$:

$$\text{Flow rate (lb/sec)} = \frac{\text{Heat Load (Btu/sec)}}{(2300°F - 2138°F)\ C_p\left(\frac{\text{Btu}}{\text{lb-°F}}\right)}$$

The resulting values for the flow rates were about 10 lb/sec. One may immediately question the effect of not being able to orifice the flow to the exact calculated value. This could easily result in having the

exit temperature difference twice as great as desired if the flow rate is higher than design value, or it could be almost zero if the flow rate were less than desired. First, it should be emphasized that there is no possibility of physical "burn-out" of the tube wall. Since there is no heat generation in the boiler, the maximum achievable temperature is that of the primary fluid at the inlet which is far below the melting temperature. However, if the flow rate is above or below its design value, the vapor quality leaving the boiler region will be slightly less than the design value. For high flow rates, the heat flux will be higher and the dry wall condition will occur at a lower quality. For low flow rates, the heat flux will be low and the total heat transfer will be less than that required to produce the design exit quality. For flow rate variations caused by inaccurate orificing, which would probably be about 3 to 5% of the total flow, the drop in exit quality would be small, less than 3 or 4% quality. This may be inferred from Fig. 8, which shows that the bulk of the change in quality occurs in the beginning and that only a small amount of heat addition occurs near the exit.

A computer code was written to perform the actual design calculations for the subcooled region and the boiling region for these designs. The details of this code are described in Appendix B. The major input numbers are the flow rate of the primary fluid, the flow rate of the working fluid, the number of tubes, the heat loads, the tube ID, and the tube spacing. The output information consists of the tube lengths and the pressure drop across the boiling section.

In the computer calculation the heated lengths in both the subcooled region and the boiling region were divided into ten sections. The length required for each section was then calculated. This procedure was required for the tapered tube designs because the overall heat transfer coefficient varied significantly from the small end to the large one. This procedure was also used for the straight tube designs for convenience. For the tapered tube designs, the required boiler length for each section was calculated by assuming that the tube ID was constant over that section. For the straight tube designs, the above assumption was exact. The pressure drop over each section in the boiling region was also calculated; the pressure drop in the subcooled

portion was neglected. Also, it should be mentioned that a trial-and-error procedure was used for the tapered tube designs. This procedure was required since the tube ID at any location could be calculated only if the total length were known.

The details of the calculations for several boiler-superheater units are given in Table 6.

Table 6. Low Entrainment Design Procedure

Line Number	Item	Source	Potassium	Potassium	Cesium	Cesium
1	Working fluid	Given	K	K	Cs	Cs
2	Total flow rate, lb/sec	Given	2.22	2.22	8.9	8.9
3	Criterion for maximum flow per tube		Eqn. 1	Eqn. 1	Eqn. 1	Eqn. 1
4	Exit enthalpy, Btu/lb	Given	1230.5	1230.5	320	320
5	Total heat load, Btu/lb	Given	752.1	752.1	187	187
6	Tube ID at inlet, in.	Given	0.45	0.2	0.45	0.2
7	Tube ID at exit of boiling region, in.	Given	0.45	0.45	0.45	0.45
8	Total temperature drop of primary fluid (Li), °F	Given	100	100	100	100
9	Primary fluid inlet temperature, °F	Given	2300	2300	2300	2300
10	Critical heat flux, Btu/hr-ft^2	Assumed	50,000	50,000	50,000	50,000
11	Critical quality, %	Assumed	90	90	90	90
12	Operating pressure, psia	Assumed	214.3	214.3	314.6	314.6
13	Saturation temperature, °F	NRL-6246, NRL-6233	2125	2125	2125	2125
14	Liquid enthalpy, Btu/lb	NRL-6246, NRL-6233	504.92	504.92	148.83	148.83
15	Vapor enthalpy, Btu/lb	NRL-6246, NRL-6233	1223.47	1223.47	316.66	316.66
16	H_{fg}, Btu/lb	NRL-6246, NRL-6233	718.55	718.55	167.83	167.83
17	Enthalpy at exit of boiling region, Btu/lb	(14) + (11) x (16)	1151.92	1151.92	299.83	299.83
18	Heat load in superheater, Btu/lb	(4) − (17)	78.58	78.58	20.17	20.17
19	Heat load in boiling region, Btu/lb	(17) − (14)	647.0	647.0	151.0	151.0
20	Heat load in subcooled region, Btu/lb	(5) − (19) − (18)	26.52	26.52	15.83	15.83
21	Tube spacing at inlet, in.	Assumed	0.0625	0.0625	0.0625	0.0625
22	Tube spacing at exit of boiling region, in.	Assumed	0.0625	0.0625	0.0625	0.0625
23	Tube wall thickness, in.	Assumed	0.03	0.03	0.03	0.03
24	Flow area per tube, ft^2	$(\pi/4)((6)/12)^2$	0.0011	-	0.0011	-
25	Maximum flow rate per tube (for straight tubes), lb/sec-ft^2	Figs. 4 and 5	40.0	-	40.0	-

Table 6. (continued)

Line Number	Item	Source	Potassium	Potassium	Cesium	Cesium
26	Maximum flow rate per tube (for tapered tubes), lb/sec	Figs. 6 and 7	-	0.03865	-	0.03865
27	Maximum flow rate per tube (for straight tubes), lb/sec	(24) x (25)	0.04425	-	0.04425	-
28	Number of tubes	(2)/(26), (2)/(27)	51	58	201	230
29	Total primary flow rate, lb/sec	(5) x (2)/(8) x C_p	17.01	17.01	16.97	16.97
30	Primary flow rate in boiling region, lb/sec	Assumed	9.30	9.3	9.26	9.26
31	Primary flow rate in superheater region, lb/sec	(29) - (30)	7.71	7.71	7.71	7.71
32	Heat transfer area required in subcooled region, ft^2	Computer code	0.477	0.265	0.632	1.21
33	Length of subcooled region, ft	Computer code	0.0744	0.0750	0.0446	0.0479
34	Total heat transfer area in subcooled and boiling regions, ft^2	Computer code	20.04	19.37	20.29	21.28
35	Total length of subcooled and boiling regions, ft	Computer code	3.127	3.77	0.995	0.8424
36	Pressure drop across boiling region, psi	Computer code	1.52	10.18	0.474	0.0746
37	Overall heat transfer coefficient at exit of boiling region, Btu/hr-ft^2-°F	Computer code	4536	4568	4210	4242
38	Total temperature difference at exit of boiling region, °F	Computer code	11.3	11.3	11.6	11.6
39	Heat flux at exit of boiling region, Btu/hr-ft^2	Computer code	51,106	51,467	48,790	49,155
40	Fin height in superheater, in.	Assumed	0.0402	0.0402	0.0402	0.0402
41	Fin width in superheater, in.	Assumed	0.02	0.02	0.02	0.02
42	Number of fins	π x (7)/2 x (41)	35	35	35	35
43	Wetted perimeter in superheater, in.	3 π x (7)	4.212	4.212	4.212	4.212
44	Flow area in superheater tube, ft^2	$\frac{1}{144}$ [(π/4)((7))^2 - (42) x (40) x (41)]	0.000908	0.000908	0.000908	0.000908
45	Equivalent diameter of superheater, in.	4 x 144 x (44) / (43)	0.124	0.124	0.124	0.124
46	Mass flow rate in tube, lb/sec-ft^2	(26) / (44), (27) / (44)	48.75	42.6	48.75	42.6
47	h for air with same G and D_e, Btu/hr-ft^2-°F	Fig. H 5.5 of Ref. 16, (46), (45)	160	140	160	140
48	Ratio of h vapor at 2125°F to h air	$C_p^{0.4}$ $k^{0.6}/\mu^{0.4}$ x 0.169	0.6	0.6	0.22	0.22

Table 6. (continued)

Item Number	Item	Source	Potassium	Potassium	Cesium	Cesium
49	Vapor heat transfer coefficient, Btu/hr-ft^2-°F	(47) x (48)	96	84	35.2	30.8
50	Fin efficiency	Fig. H 7.3 of Ref. 16	0.98	0.983	0.99	0.995
51	Tube OD, in.	(7) + (23) x 2	0.51	0.51	0.51	0.51
52	Center-to-center tube spacing, in.	(51) + (22)	0.5725	0.5725	0.5725	0.5725
53	Equivalent diameter on shell side, in.	(51) $[1.102\ ((52)/(51))^2 - 1]$	0.199	0.199	0.199	0.199
54	Ratio of thermal conductivity of primary fluid to D_e, Btu/hr-ft-°F-in.	k/(53)	148.5	148.5	148.5	148.5
55	Flow area for primary fluid per tube, ft^2	$\frac{2}{144}$ $[0.433\ ((52))^2 - 0.39\ ((51))^2]$	0.000564	0.000564	0.000564	0.000564
56	G C_p for primary fluid in superheater, Btu/sec-ft^2-°F	(31) x C_p/(28) x (55)	263	231	66.7	58.3
57	Primary fluid heat transfer coefficient, Btu/hr-ft^2-°F	Fig. H 5.15 of Ref. 16, (56), (54)	18,000	17,000	14,000	13,000
58	Resistance in primary fluid, hr-ft^2-°F/Btu	1/(57)	0.556×10^{-4}	0.588×10^{-4}	0.714×10^{-4}	0.769×10^{-4}
59	Tube wall thermal conductivity, Btu/hr-ft-°F	Given	35	35	35	35
60	Tube wall resistance, hr-ft^2-°F/Btu	(23)/12 x (59)	0.71×10^{-4}	0.71×10^{-4}	0.71×10^{-4}	0.71×10^{-4}
61	Thermal resistance of vapor side, hr-ft^2-°F/Btu	(51)/(50) x (7) x (49)	39.4×10^{-4}	45×10^{-4}	107.4×10^{-4}	122.6×10^{-4}
62	1/U, hr-ft^2-°F/Btu	(58) + (60) + (61)	40.666×10^{-4}	46.298×10^{-4}	108.824×10^{-4}	124.079×10^{-4}
63	Temperature at exit of superheater, °F	Given	2125	2125	2125	2125
64	Temp. difference at exit of superheater, °F	(9) - (63)	150	150	150	150
65	Primary fluid temp. at superheater inlet, °F	(9) - (18) x (2) x 3600/(31) x C_p	2275.6	2275.6	2275	2275.2
66	Temp. difference at superheater inlet, °F	(65) - (13)	150	150	150	150
67	LMTD in superheater, °F	Fig. H 4.1 of Ref. 16	150	150	150	150
68	Heat transfer area required for superheater, ft^2	(18) x (2) x 3600 x (62)/(67)	16.95	19.30	46.53	46.53
69	Heat transfer area per foot of superheater, ft^2	(28) x π ((51))^2/144	6.8	7.74	26.8	30.7
70	Superheater length, ft	(68)/(69)	2.49	2.49	1.734	1.734
71	Reynolds Number in superheater	(46) x (45)/12 x μ	3.26×10^4	2.85×10^4	2.74×10^4	2.4×10^4

Table 6. (continued)

Item Number	Item	Source	Potassium	Potassium	Cesium	Cesium
72	Friction factor	Fig. H 3.4 of Ref. 16	0.025	0.026	0.026	0.027
73	Friction pressure drop in S/H, psi	(72) x ((46))^2 x (70) / (45) x 2gρ 144	0.092	0.083	0.013	0.013
74	Momentum pressure drop in boiler, psi	Fig. H 3.3 of Ref. 16	0.7	0.52	0.09	0.68
75	Density of structure material, gm/cc	Assumed	8.9	8.9	8.9	8.9
76	Center-to-center tube spacing (inlet/outlet), in.	(7) + 2 x (23) + (22)	0.5725	0.5725 /0.3225	0.5725	0.5725 /0.3225
77	Shell inside radius, in.	Fig. H 6.3 of Ref. 16 (76)	2.29	1.45/2.58	4.58	2.74/4.87
78	Pressure on primary side, psi	Assumed	50	50	50	50
79	Pressure on vapor side, psi	Assumed	250	250	350	350
80	Design pressure difference for header sheets, psi	(79) − (78)	200	200	300	300
81	S_{max} x t^2/P x r^2 for header sheet	Fig. H 8.2 of Ref. 16 (76)	7.5	4.75/7.5	7.5	4.75/7.5
82	Header sheet thickness, in.	(88) x (77) x $\sqrt{2}$ (81) $/2S_{max}$ Sin 45°	0.526	0.5/0.588	1.54	1.04/1.63
83	Volume of holes in header sheet, ft^3	(28) π((51))^2 x (82) /4 x 1728	3.18 x 10^{-3}	0.0089/0.0403	0.0366	0.073/0.0443
84	Metal volume in header sheet, ft^3	π[($\frac{\pi}{2}$ (77) /Sin 45°)^2 x (82) / 1728] − (83)	3.02 x 10^{-3}	0.0144/0.046	0.0364	0.102/0.0419
85	Weight of header sheet, lb	(75) x 62.4 x (84)	0.526	0.79/2.53	20.2	5.5/23.2
86	Header thickness, in.	(79) x (77) /2 x S_{max}	0.147	9.3x10^{-2}/0.17	0.411	0.25/0.44
87	Header weight, lb	2 π((77))^2 x (86) x (75) x 62.4/1728	1.55	0.40/2.2	17.4	3.73/20.9
88	Shell thickness, in.	(78) x (77) /S_{max}	0.0587	3.7x10^{-2}/ /6.6x10^{-3}	0.117	7.0x10^{-2} /0.125
89	Shell weight for straight tube, lb	2π (77) x (88) x((35) + (70) + 2 x (82))x (75) x 62.4/1728	19.4	-	44.18	-
90	Shell weight for tapered tube (in superheater), lb	2π (77) x (88) x ((70) + (82))x (75) x 62.4/1728	-	16.9	-	11.4
91	Shell weight for tapered tube (in boiling and subcooled region), lb	π(r_1+r_2) $\sqrt{(35)^2+(r_1-r_2)^2}$ x (88) x (75) x 62.4/1728	-	2.7	-	26.2
92	Equivalent tube thickness in superheater, in.	(23) + ((40) x (41) x (42))/π x (7)	0.05	0.05	0.05	0.05
93	Weight of tubes, lb	[(23) x (34) + (92) x (68)] (75) x 62.4/12	86.9	93.7	192.0	79.2
94	Total dry weight	2 x (85) + 2 x (87) + (89) + (90) + (91)	112.7	119.9	309	304.0
95	Total wet weight	(94) + Lithium volume x ρ_{Li} + $\frac{2}{3}$ π ((77))^3 $\rho_{working\ fluid}$	120.2	129.3	331.7	319.0

Weight Estimation

The boiler weights for the designs of Table 8 were estimated on the basis of the precepts listed in Table 7.

Table 7. Precepts for Weight Estimation

1. The density of the structural material was taken as 8.9 gm/cm^3.
2. Figure H 6.3 of Ref. 16 was used to estimate the header sheet radius.
3. The pressure of the primary fluid was taken as 50 psi.
4. The pressures of cesium and potassium were taken as 350 and 250 psi, respectively.
5. The maximum allowable stress, S_{max}, was taken as 1950 psi.
6. The header sheet was assumed to be a segment of a spherical shell with an included cone angle of 90°.

$$t = \frac{P\ r/\mathrm{Sin}\ 45^\circ}{2\ S_{max}} \times \sqrt{2.a}$$

where a is $\frac{S_{max}\ t^2}{P\ r^2}$ obtained from Fig. 8.2 of Ref. 16.

7. The header casing was taken as hemispherical.
8. The header casing thickness was taken as $t = \frac{P \times r}{2 \times S_{max}}$
9. The shell thickness was taken as $t = P \times r/S_{max}$.

Table 8. Summary of Data for Boiler Designs

Major Reference Designs									Low Entrainment Potassium		Vortex Potassium			Vortex Cesium	Low Entrainment Cesium
Boiler Number →	1	2	3	4	5	6	7	8	9	10	11	12	13	14	15
	Tapered Tube Boiler of ORNL-TM-1366 (Counter Flow)	Straight Tube AiResearch Boiler (Parallel-Flow)	Straight Tube Boiler of NASA-CR-842 (Counter Flow With Vortex Generator)	Straight Tube Boiler of NASA-CR-842 (Counter Flow Without Vortex Generator)	Straight Tube Boiler (Boiler Exit Quality of 97%)	Straight Tube Boiler (Boiler Exit Quality of 90%)	Tapered Tube Boiler (Boiler Exit Quality of 97%)	Tapered Tube Boiler (Boiler Exit Quality of 90%)	Tapered Tube Boiler (Boiler Exit Quality of 90% With Tube Bend in Superh.	Straight Tube Boiler (Boiler Exit Quality of 97% For Low G)	Straight Tube Boiler (Counter-Flow With Vortex Generator)	Straight Tube Boiler (Boiler Exit Quality of 90%)	Tapered Tube Boiler (Boiler Exit Quality of 90%)	Straight Tube Boiler (Counter-Flow With Vortex Generator)	Tapered Tube Boiler (Boiler Exit Quality of 90% with Tube Bend in Superh.
	Potassium	Potassium	Potassium	Potassium	Potassium	Potassium	Potassium	Potassium	Potassium	Potassium	Potassium	Cesium	Cesium	Cesium	Cesium
1. Thermal output, Mw	2.2	0.3	8.3	8.3	1.76	1.76	1.76	1.76	1.76	1.76	1.76	1.76	1.76	1.76	1.76
2. Thermal output per tube, kw/tube	12.5	15.8	32.7	32.7	34.5	34.5	30.7	30.7	30.7	17.6	88	8.76	7.65	39.1	7.65
3. Vapor density at exit, lb/ft^3	0.226	0.0757	0.25	0.25	0.361	0.361	0.361	0.361	0.361	0.361	0.361	1.905	1.905	1.905	1.905
4. Vapor velocity at exit, ft/sec	50	515	56.8	56.8	132	132	116	116	116	67.3	83.0	25.6	22.3	26.6	22.3
5. Vapor flow rate (total), lb/sec	2.72	0.2	9.36	0.36	2.22	2.22	2.22	2.22	2.22	2.22	2.22	8.9	8.9	8.9	8.9
6. Vapor flow passage exit area, ft^2	0.24	0.00513	0.659	0.659	0.0463	0.0463	0.0527	0.0527	0.0527	0.0908	0.074	0.1827	0.209	0.1755	0.209
7. Tube ID at inlet, in.	0.3	0.2525	0.69	0.69	0.45	0.45	0.2	0.2	0.2	0.45	0.75	0.45	0.2	0.75	0.2
8. Tube ID at outlet, in.	0.5	0.2525	0.69	0.69	0.45	0.45	0.45	0.45	0.45	0.45	0.75	0.45	0.45	0.75	0.45
9. Number of tubes	176	19	254	254	51	51	58	58	58	100	19	201	230	45	230
10. Area required in subcooled region, ft^2					0.476	0.477	0.263	0.265	0.265	0.485	1.955	1.21	0.632	3.86	0.632
11. Area required in boiling region, ft^2					26.936	19.56	26.251	19.11	19.11	28.096	30.8	20.07	19.685	27.0	19.685
12. Area required in superheater, ft^2					5.862	16.952	6.671	19.30	7.75	11.023	3.525	46.53	53.08	9.8	35.0
13. Total heat transfer area, ft^2		6.18			33.274	36.99	33.18	38.67	27.13	39.604	36.28	67.81	73.37	40.66	55.3
14. Length of subcooled region, ft			0.291	0.258	0.0743	0.0744	0.0749	0.0750	0.0750	0.0386	0.508	0.0479	0.0446	0.424	0.0446
15. Length of boiling region, ft			2.19	11.4	4.203	3.053	5.186	3.7	3.7	2.236	8.0	0.795	0.95	3.00	0.95
16. Length of superheater, ft			3.15	9.65	0.861	2.49	0.862	2.49	1.0	0.826	0.87	1.727	1.728	1.075	1.14
17. Total boiler length, ft	4.4	4.1	5.66	21.31	5.138	5.617	6.123	6.27	4.775	3.1	9.378	2.57	2.723	4.5	2.13
18. Tube wall thickness, in.		0.03	0.03	0.03	0.03	0.03	0.03	0.03	0.03	0.03	0.03	0.03	0.03	0.03	0.03
19. Primary fluid temperature at inlet, °F	2000	1800	2200	2200	2300	2300	2300	2300	2300	2300	2300	2300	2300	2300	2300
20. Primary fluid temperature at exit, °F	1900	1700	2050	2050	2200	2200	2200	2200	2200	2200	2200	2200	2200	2200	2200
21. Working fluid temperature at inlet, °F	1800	1100	1200	1200	2005	2005	2005	2005	2005	2005	2005	1850	1850	2005	1850
22. Working fluid temperature at exit, °F	1850	1600	2150	2150	2150	2150	2150	2150	2150	2150	2150	2150	2150	2150	2150
23. Design pressure in boiler		38.2	150	150	214.3	214.3	214.3	214.3	214.3	214.3	214.3	314.6	314.6	314.6	314.6
24. Friction pressure drop in boiling region, psi		18	0.6		2.04	1.52	20.1	10.20	10.20	0.11	44.0	0.075	0.474	51.2	0.474
25. Friction Pressure drop in superheater, psi					0.032	0.09	0.29	0.08	0.04	0.018	2.7	0.013	0.011	1.72	0.007
26. Momentum pressure drop , psi					0.7	0.7	0.52	0.52	0.52	0.17	0.23	0.09	0.068	0.27	0.068
27. Total pressure drop, psi	16.0				2.77	2.31	20.91	10.8	10.76	0.3	25.73	0.178	0.553	33.7	0.549
28. Average heat flux, Btu/hr-ft^2	85,000	160,000	110,000	30,000	180,500	162,500	181,000	155,000	221,000	151,600	165,400	88,700	81,500	147,600	109,000
29. Heat flux at exit of boiler region, Btu/hr-ft^2					20,608	51,106	20,878	51,467	51,467	19,757		48,790	49,155		49,155
30. Total boiler volume, ft^3					0.586	0.642	0.596	0.696	0.613	0.796	3.19	1.175	1.2	2.32	0.783
31. Shell inside radius (inlet/outlet), in					2.29	2.29	1.45/2.56	1.45/2.56	1.45/3.85	3.435	4.025	4.58	2.74/4.87	4.84	2.74/7.32
32. Shell thickness, in.					0.0587	0.0587	0.0661	0.0661	0.0661	0.0881	0.103	0.117	0.128	0.124	0.0938
33. Shell weight, lb					17.8	19.4	19.6	20	19.0	26.4	97.9	44.2	37.6	73.9	21.5
34. Head thickness (inlet/outlet), in.					0.148	0.148	0.093/0.165	0.093/0.165	0.093/0.246	0.79	0.258	0.411	0.25/0.44	0.434	0.25/0.562
35. Head weight (inlet/outlet), lb					1.55	1.55	0.396/2.21	0.396/2.21	0.396/10.32	5.25	8.44	17.4	3.73/20.9	20.5	3.73/30.2
36. Header sheet thickness (inlet/outlet), in.					0.526	0.526	0.5/0.588	0.5/0.588	0.5/1.0	0.79	0.64	1.54	1.04/1.63	1.08	1.04/1.0
37. Header sheet weight (inlet/outlet), lb					1.66	1.66	0.79/2.53	0.79/2.53	0.79/4.1	6.34	10.8	20.2	5.5/23.2	20.7	5.5/15.1
38. Tube weight, lb					58.42	86.9	60	93.9	53.9	77.9	63.0	192	213.0	67.6	150
39. Total dry weight, lb					82.7	112.7	85.6	119.9	88.5	122.0	199.4	309	304.0	224.3	226.1
40. Total wet weight, lb					89.5	120.2	87.9	129.3	99.1	134.0	278.0	331.7	319	282.3	234.5

RESULTS AND DISCUSSION

The results of the design calculations for a variety of boundary conditions are summarized in Table 8. Note that a major variable was the quality at the exit of the boiling region (which then determined the heat flux giving a dry wall condition). In addition, several criteria were employed for the maximum allowable vapor velocity to avoid liquid entrainment, and both straight and tapered tubes were considered.

Vortex Generator Approach

The designs using the vortex generator inserts are given as Boilers No. 11 and 14 of Table 8 for potassium and cesium, respectively, and a layout of Boiler No. 11 is given in Fig. 13. For comparison of these design calculations with a unit that has been operated, test data for an AiResearch boiler (see Refs. 3 and 4) are included under Boiler No. 2. Assuming that the product of the overall heat transfer coefficient and the LMTD are approximately the same, the required heat transfer area would be proportional to the heat load. On this basis the AiResearch boiler may be compared to Boiler No. 11 which is similar. By multiplying the total area for the AiResearch boiler (6.18 ft^2) by the ratio of the heat loads (1.76/0.3), the result is 36.6 ft^2 as compared to the design value 36.28 ft^2. This comparison gives confidence in the calculations listed in Table 8.

The cesium boiler has a dry weight of about 224 lb while that for potassium is 200 lb. (The corresponding wet weights are 282 lb and 278 lb, respectively.) The design procedure entailed varying the tube spacing until the average heat flux in the boiling region (from 0 to 100% quality) was less than 200,000 Btu/hr·ft^2 (to be consistent with Ref. 5 and Fig. 3 of this report). For the vortex generator designs described in Table 8, a spacing of 0.8 in. was used for the potassium while that for cesium was 0.4 in. The resulting average heat flux from 0 to 100% quality was 186,000 Btu/hr-ft^2 for potassium and 197,000 btu/hr-ft^2 for cesium. This indicates that the potassium design could be improved by reducing the spacing. For a proper comparison between the weights of the cesium and potassium boilers, both designs should have the same average heat flux. An additional potassium

design was prepared with a spacing of 0.4 in. These results are as follows:

Table 9. Potassium Boiler Weights for Vortex Generator Design

Spacing (in.)	Average Heat Flux 0 to 100% (Btu/hr-ft^2)	Weight Wet (lb)
0.8	186,000	278
0.4	256,000	102.4

By linear interpolation between the above two cases, it was estimated that a potassium boiler with an average heat flux (0 to 100% quality) of 197,000 Btu/hr-ft^2 would have a wet weight of about 175 lb. This indicates that the ratio of the boiler wet weight for cesium to that for potassium is 224/175 = 1.28. From a previous study,[22] a value of 1.65 was obtained for this ratio for designs using vortex generator inserts.

The weight of this vortex design may be compared to the low entrainment design for boiler No. 9 of Table 8. This ratio is 175/99.1 = 1.78.

The overall pressure drop across the above four cesium and potassium boilers range from about 1% to 15% of the boiler pressure. It is believed at ORNL that satisfactory flow stability could be obtained in the tapered tube boilers with some supplemental orificing at the tube inlets for pressure drops as low as 5%, but the low entrainment cesium boiler (No. 15 of Table 8) has a pressure drop that is less than 1% of the boiler pressure, and this is probably too low. To increase it, the number of tubes would have to be reduced together with the exit design vapor quality. Time did not permit further study.

Low Entrainment Approach

The characteristics of a typical boiler designed on the basis of the low entrainment approach are shown in Fig. 10. Seventy-five percent of the total evaporation is completed in less than half of the boiler length. This condition results from using parallel flow to keep the heat flux low near the boiler outlet and thus increasing the quality for the transition

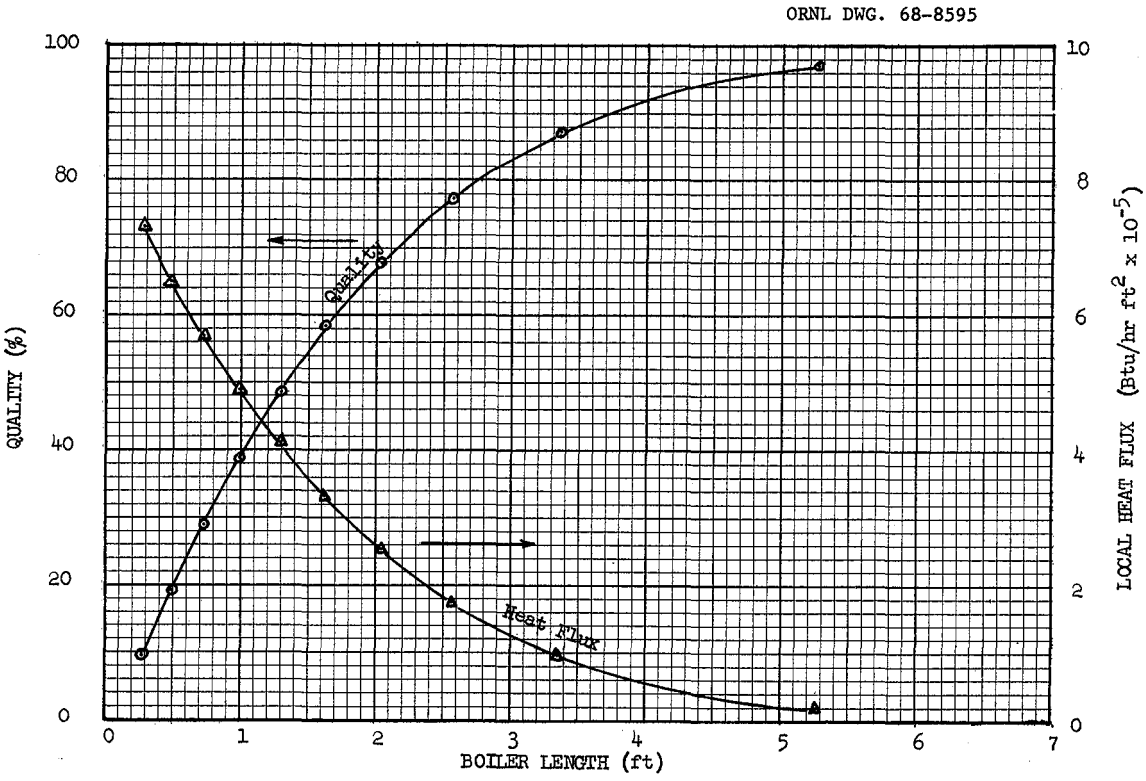

Fig. 10. Heat Flux and Quality as a Function of Boiler Length for Boiler Number 7.

from annular flow to a dry wall condition. Thus, using a low heat flux requires a longer boiler length. Intuitively, one might expect that a nearly optimum design would result when the boiling region is terminated at the point where the heat flux in the boiling region is equal to that available in the superheater. To investigate this problem, several values for the design quality at the exit of the boiling region were chosen. The results for potassium are shown in Fig. 11, and those for cesium are shown in Fig. 12. For the tapered tube potassium boiler, the minimum overall tube length is obtained for a boiler exit quality of about 94%. The corresponding value for cesium would be about 98%.

A possible improvement over these designs occurs when the design quality is set at 90%. The boiling length required for a tapered tube potassium design is 3.75 ft. The superheater length is 2.49 ft, calculated on the basis of simple forced convection gas heated transfer relations. However, if the superheater tube is bent 180 deg, ORNL work on vapor separators indicates that over 99% of the entrained droplets would be centrifuged to the wall where they would be quickly vaporized. Thus the superheater length probably can be reduced to about 1.0 ft as a consequence of the improved heat transfer obtained by centrifuging the moisture to the wall in the bend. This design advantage was considered, and the results are tabulated as Boiler No. 9 of Table 8. In this case, it was assumed that dry saturated vapor entered the straight portion of the superheater immediately downstream of the bend.

Preliminary layouts for Boiler Nos. 8 and 9 (with and without credit for the improved heat transfer in the bend) are shown in Figs. 14 and 15, respectively. The design taking credit for the improved heat transfer in the bend gives a weight reduction of about 70 lb. For comparison between the weights of the cesium and the potassium boilers, the 90% quality cases for tapered and straight tubes were used. For the 90% straight tube case the ratio of the weight for cesium to that for potassium is 309/113 or 2.73; for the tapered tube case, this is 319/120 or 2.66.

The J tube configuration was also considered for the cesium system. This design is reported as boiler No. 15 in Table 8. The amount of superheat achieved in the tube length necessary for a full 180° bend was significantly larger than the required 25°F. Thus, the boiler weight could be reduced by considering a bend of less than 180°F.

The above results apparently stem from several effects. For the minimum entrainment approach, the vapor heat transfer coefficient for

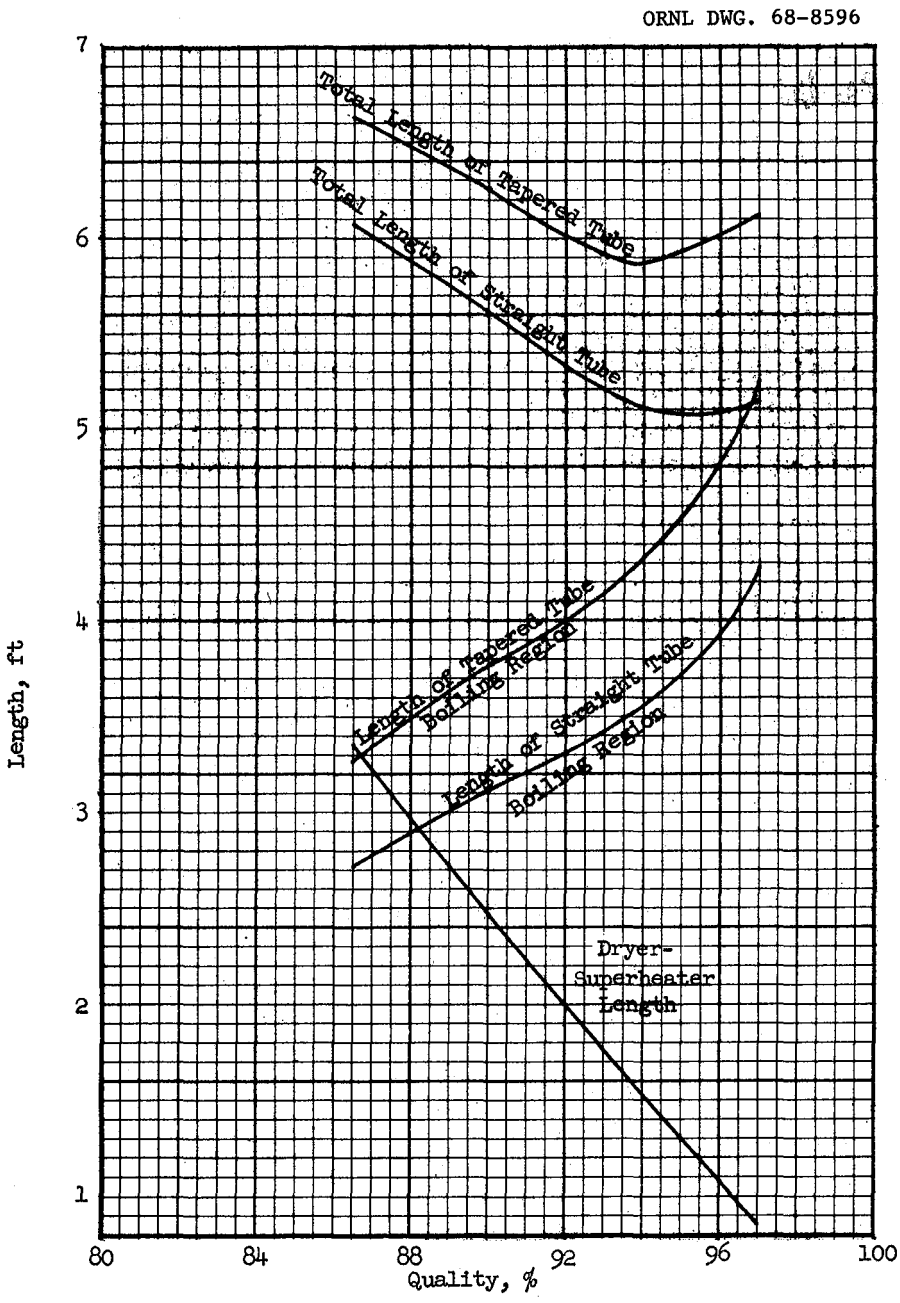

Fig. 11. Effect of Design Quality at Exit of Boiling Region on Potassium Boiler Length.

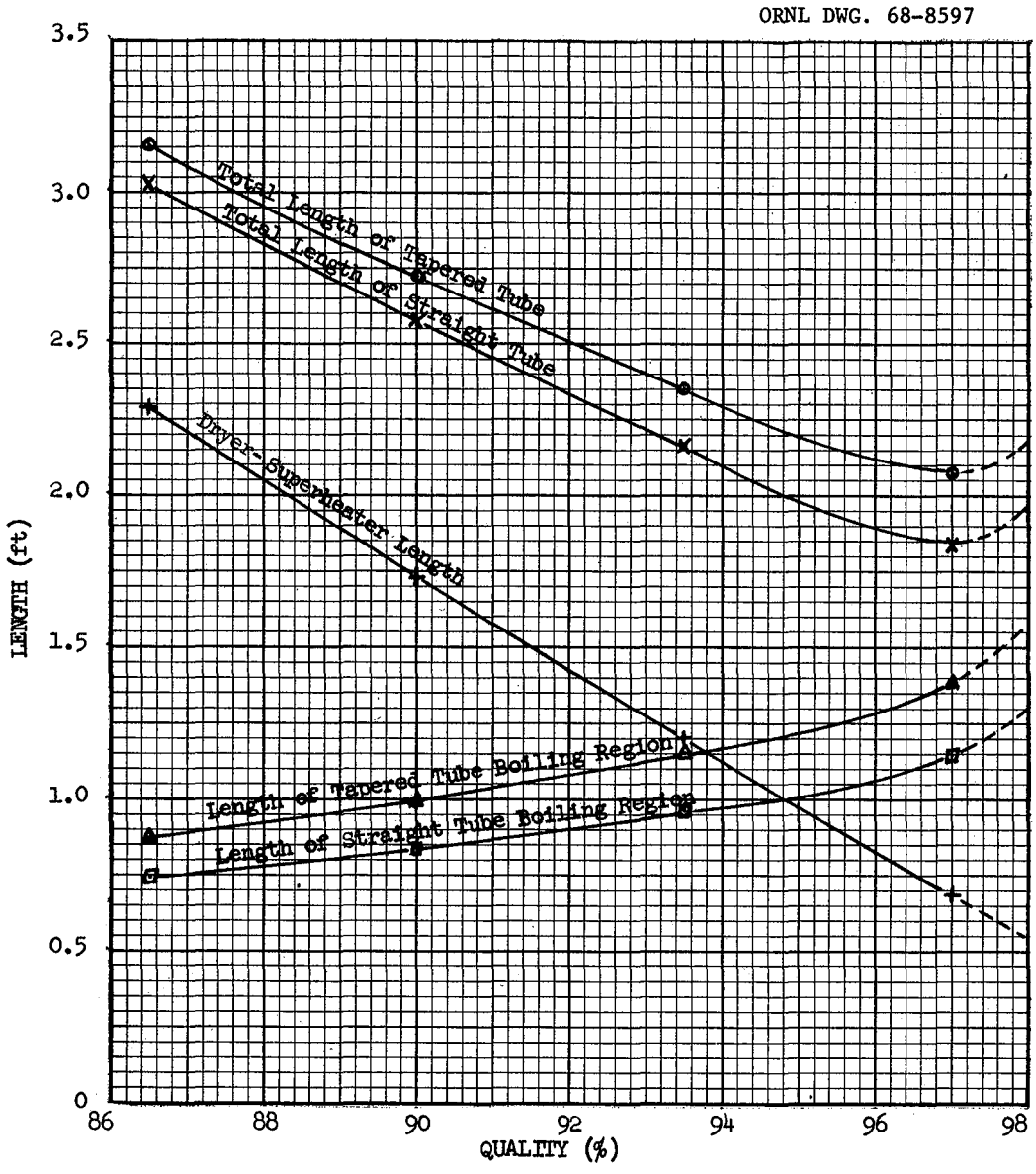

Fig. 12. Effect of Design Quality at Exit of Boiling Region on Cesium Boiler Length.

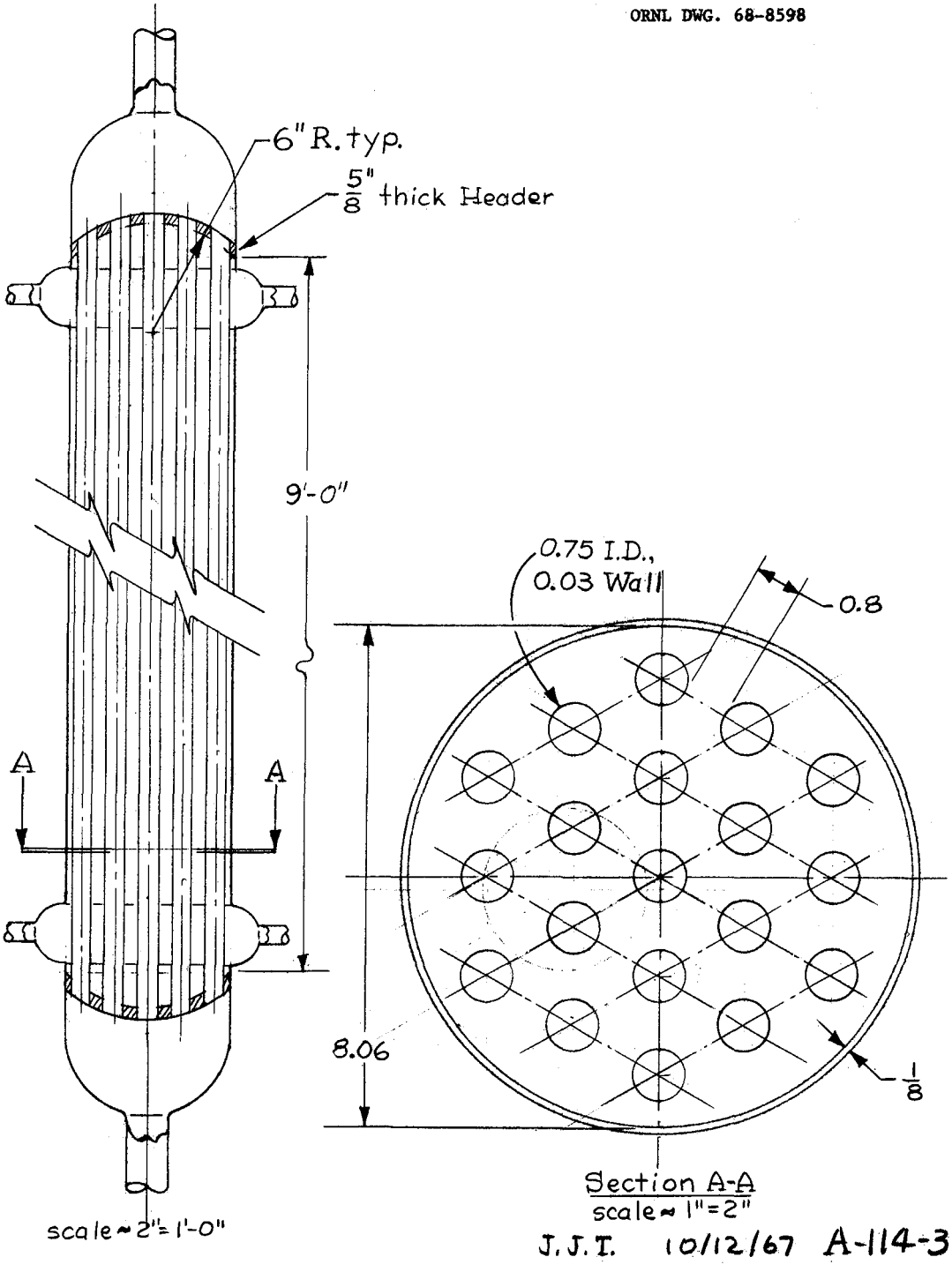

Fig. 13. Layout of Boiler Number 11.

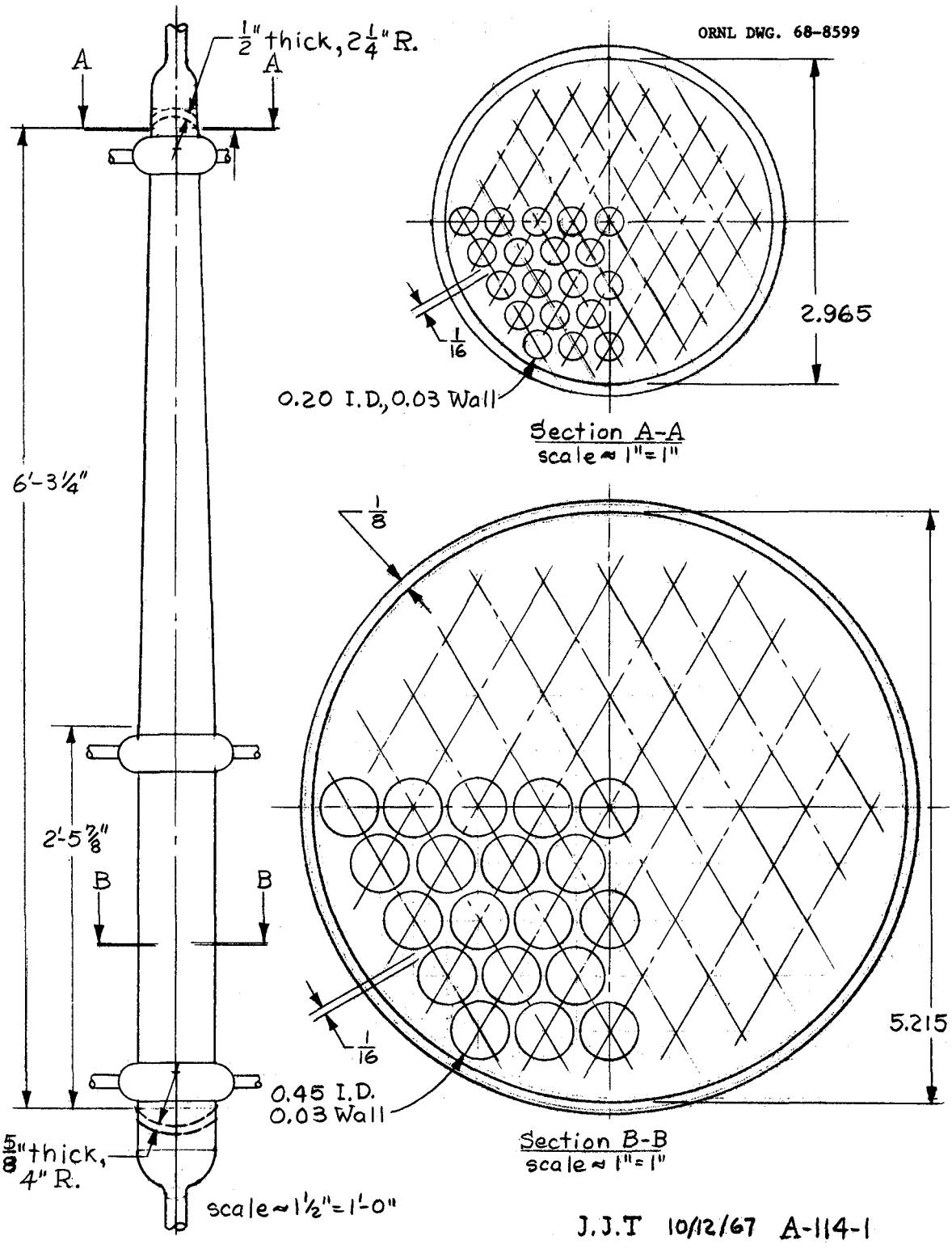

Fig. 14. Layout of Boiler Number 8.

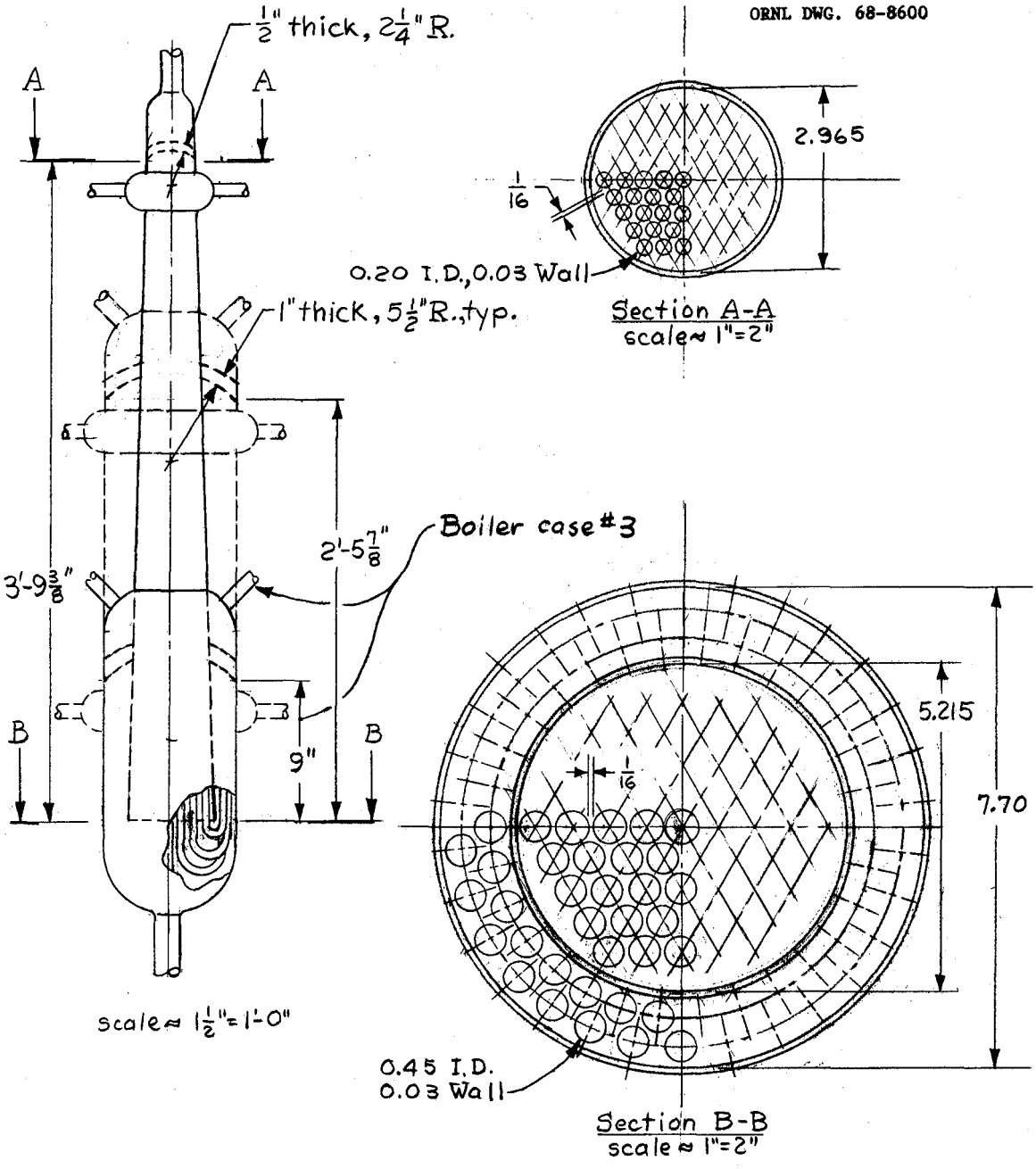

J.J.T. 10/12/67 A-114-2

Fig. 15. Layout of Boiler Number 9.

cesium is about one-third that of potassium. This requires more superheater area for cesium than for potassium, and thus increases the weight difference. Also, the Chien and Ibele criterion indicates that the mass velocity for potassium and cesium are about equal. Since the total flow rate of cesium is higher than that for potassium, the cesium systems require more tubes and thus the shell radius is larger. With a larger shell radius, the header sheets, headers, and shell must all be larger, thicker, and thus heavier. For the vortex generator design, the number of tubes for the cesium boiler was also greater than that for potassium. This requirement was also caused by the higher cesium mass flow rate; the number of cesium boiler tubes was made as small as possible in light of pressure drop considerations. Again, the larger number of tubes resulted in a larger shell radius and thus more weight.

The above cases were designed using the Chien and Ibele criterion for the maximum vapor velocity. Boiler No. 10 was designed using Mozharov's criterion.[13] This case may be compared to that of Boiler No. 5. These results indicate that the more severe criterion would increase the boiler weights by a factor of 122/83 or 1.47.

PART LOAD AND TRANSIENT CHARACTERISTICS

The design calculations presented above were based on steady state operation at full power. Since the system will operate at part load during most of its life, the part load characteristics of the proposed designs are important. Also since load changes are anticipated, transient operation should be considered. These conditions have been investigated for one cesium and several potassium boilers.

In order to estimate the above characteristics, the system control scheme must be specified. Various approaches to system control are discussed in a companion report on system integration, and one is shown to be the most promising of the several considered. The main features of this control scheme pertinent to the boiler operation are outlined in Table 10 and Fig. 16. Based on these precepts, the relations between the temperature and pressure of the vapor at the turbine inlet and the

Table 10. System Control Scheme

1. Vary the Rankine cycle working fluid feed flow rate to the boiler to maintain a constant turbine speed (the flow rate will be proportional to the load.)

2. The relation between the working fluid flow rate and its temperature and pressure at the inlet to the turbine for part load operation will be approximately

$$w\frac{\sqrt{T}}{P} = c$$

where

w = weight flow rate, lb/sec

T = temperature, °R

P = pressure, psi

c = a constant, 0.528 for the potassium system

3. The saturation temperature and pressure in the boiler at part load will be approximately the values indicated in (2) (neglecting the pressure drop).

4. The temperature at the turbine inlet will be measured to indicate the load.

5. The reactor controls will be operated to vary the reactor outlet temperature according to a schedule that will depend on the indicated load.

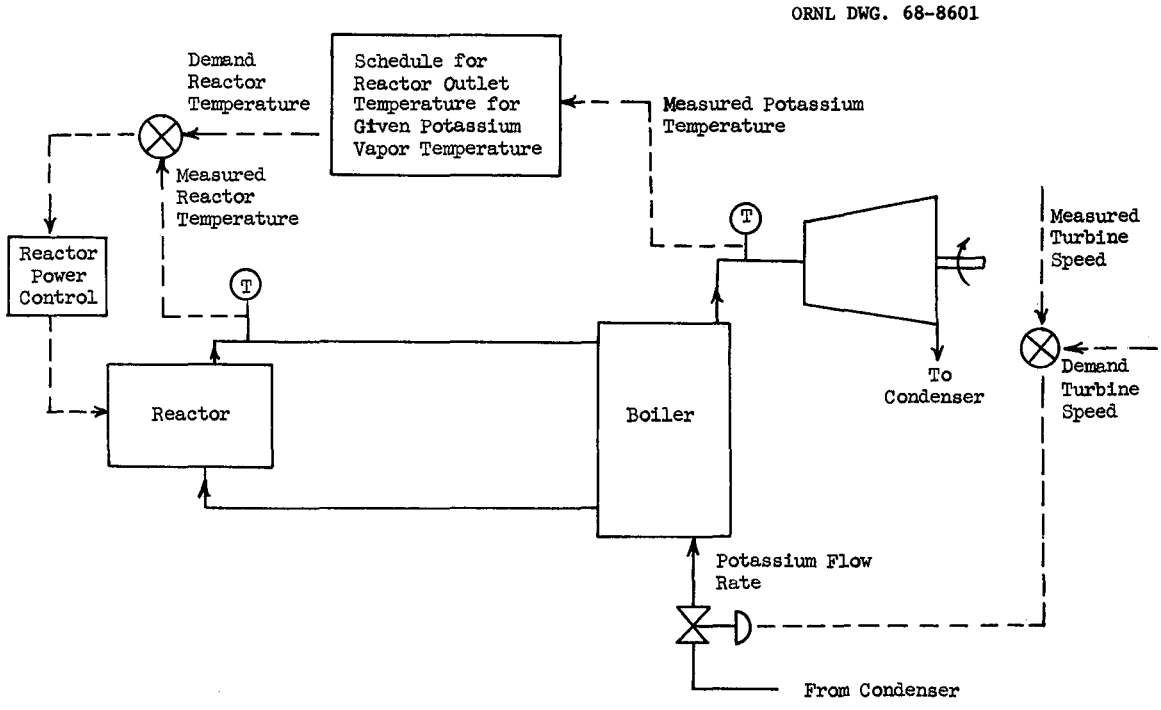

Fig. 16. System Control Scheme.

flow rate for part load conditions were calculated and plotted in Fig. 17 for the potassium system. The problem now is to determine a proper choice for the scheduled reactor outlet temperature that will result in reasonable part load operation.

Another set of considerations is presented by the effects of rapid changes in load. A rapid change in electrical load, up or down, will cause a correspondingly rapid change in the potassium flow rate. This will result in a rapid change in the temperature of the vapor at the boiler exit. The reactor system will respond by changing the reactor outlet temperature. However, owing to the thermal inertia of the reactor system, a significant delay time (of the order of many seconds) will be encountered before the reactor outlet temperature can reach the scheduled value for the new condition. Thus, during the initial phase of the transient, some moisture may be present in the vapor entering the turbine which, if it is large, may cause damage. The worst possible case is that for an infinite reactor system delay time. This case may be evaluated by using a steady state analysis considering the reactor outlet temperature to have its initial value while the potassium loop operates at the new flow rate. This is equivalent to considering the effects of a load change with the control scheme for the reactor outlet temperature inoperable.

Vortex Generator Part Load Analysis

The procedure used for the steady state design for full power was based on Fig. 3. For the present purpose a more detailed method based on the equations listed in Appendix A was used. The subcooled region was neglected in this calculation. The procedure was first to assume a value for the lithium temperature at the potassium inlet end. The potassium temperature at the inlet was obtained from Fig. 17 after selecting the load (i.e., the potassium flow rate). Thus, by knowing the temperature difference and assuming a boiling heat transfer coefficient of 10,000 Btu/hr-ft^2 (and using the same lithium and tube wall thermal resistance as the original design), the heat flux was calculated. This value was assumed constant over a 0.5 ft^2 area of the boiler. By

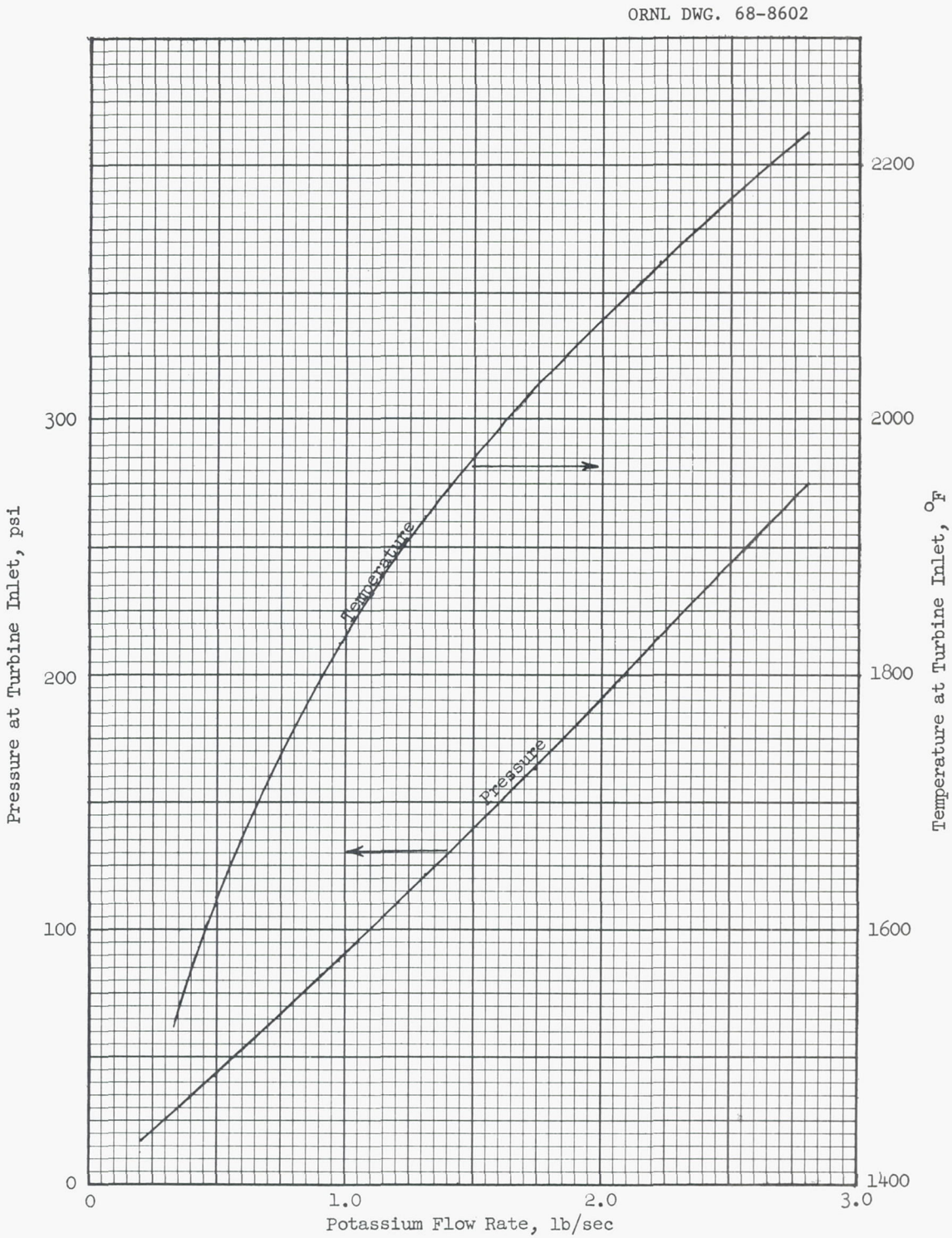

Fig. 17. Turbine Inlet Pressure and Temperature as a Function of Potassium Flow Rate.

multiplying the heat flux by 0.5 ft^2, the total heat transfer through that area was obtained. From this value the change in potassium quality and the decrease in lithium temperature over this area were calculated. At this point a new temperature difference was calculated and the process was repeated for the next 0.5 ft^2 area of the boiler. At each point the heat flux was compared to a transition heat flux which was calculated as

$$q'' = (1 - x) \times 850{,}000 \text{ Btu/hr ft}^2$$

where x is the quality. This is an approximation to Fig. 9. Once the local heat flux was greater than q", the heat-transfer coefficient on the potassium side was calculated according to the transition heat-transfer coefficient as:[23]

$$\frac{\left(\frac{h_{TB}}{hv} - 1\right)}{(1 + a_R)^{1/5}} = \frac{2.55 \times 10^5 \left(\frac{1 - x}{x}\right)^{0.7}}{(\Delta T)^2}$$

where

h_{TB} = transition boiling heat-transfer coefficient, Btu/hr ft^2 °F

h_v = vapor phase heat transfer coefficient assuming all-vapor flow at the total mass velocity, Btu/hr-ft^2-°F

a_R = radial acceleration in g's, (see Appendix A)

x = quality

ΔT = Temperature difference from tube wall to bulk fluid, °F

When the quality was equal to or greater than one, the pure vapor heat transfer coefficient was used and the heat addition was used to calculate the increase in the temperature of the potassium vapor.

After the total boiler heat transfer area was considered, the temperature of the lithium at the potassium exit end of the boiler was noted. If this was not the desired value, the procedure was repeated with a corrected guess for the lithium temperature at the potassium inlet end.

The above procedure was developed as a computer code for the CEIR remote access computer. A listing of this code appears in Appendix C.

The results from the above analysis are tabulated in Table 11.

Table 11. Part Load Conditions For the Vortex Generator Design of Boiler No. 10

	Reactor Exit Temperature	Potassium* Quality Boiler Exit	Potassium Temperature at Boiler Exit
	(°F)		(°F)
1. Steady state at 100% power	2300	1.008	2151.6
2. Step increase of 10% full power from steady state at 100% power	2300	0.814	2160
3. Steady state at 60% power	2093	1.055	2063.9
4. Step increase of 10% full power from steady state at 60% power	2093	.937	1985.
5. Steady state at 60% power	2123	1.064	2098.9
6. Step increase of 10% full power from steady state at 60% power	2123	1.025	2052

*Quality greater than 1.00 indicates superheat.

Low Liquid Entrainment Part Load Analysis

The part load characteristics for these designs were calculated using a procedure similar to that for the vortex generator design. The code used for these calculations is listed in Appendix C. The precepts for these calculations are tabulated in Table 12. The procedure is straight-forward except for calculating the effective heat transfer coefficient in the bend. It is expected that the radial acceleration produced by the bend will force the liquid droplets to the tube wall and

Table 12. Precepts for Part Load Calculations for Low Entrainment Design.

---

1. Neglect the subcooled region.

2. The heat transfer area in boiler region (parallel-flow) is 19.1 ft^2; the area in the bend of the superheater is 2.66 ft^2; the area in the straight portion of the superheater is 5.09 ft^2.

3. The lithium flow rate is 9.3 lb/sec in the parallel-flow region, and 7.71 lb/sec in the counterflow region.

4. The overall heat transfer coefficient is 4700 Btu/hr ft^2°F in the boiling region upstream of the dry wall condition.

5. The heat transfer coefficient in the transition region is:[23]

$$\frac{\left(\frac{h_{TB}}{h_v} - 1\right)}{(1 + a_R)^{1/5}} = \frac{2.55 \times 10^5 \left(\frac{1 - x}{x}\right)^{0.7}}{(\Delta T)^2}$$

x = quality

ΔT = temperature difference from bulk to wall, °F

a_R = radial acceleration in g's; equal to the square of the tangential liquid velocity divided by the product of the radius of curvature and the acceleration of gravity; g = 32.2 ft/sec^2.

h_v = vapor heat-transfer coefficient for 100% quality and total flow.

6. a_R = 0 for straight tube;

7. For the bend, a_R is given by:

$$a_R = \frac{V_T^2}{g\, r}$$

Assume: r = 1.2" = .1 ft (average for bundle)

$$V_T = \frac{(\text{vapor velocity at 100\% flow})(w/2.22)}{\sqrt{\frac{\rho_f}{\rho_g}}}$$

Table 12 (Continued)

w = total flow, lb/sec = 2.22 lb_m/sec for 100% power

$\sqrt{\frac{\rho_f}{\rho_g}}$ ≐ ratio of vapor velocity to liquid velocity ≐ 14.1

Thus, $a_R \doteq 4.25\ w^2$

8. Test for dry wall condition may be neglected from 0 to 30% quality. From 30 to 100% quality the following relation is used:

$$q'' = 850{,}000\ (1 - x)$$

will increase the heat-transfer coefficient. The heat-transfer coefficient in the transition region with radial acceleration developed by twisted tapes was correlated by Peterson[23]. This correlation was used for estimating the heat transfer coefficient with radial acceleration developed by the tube bend as a first approximation. The results of these calculations are shown in Table 13.

Discussion of Part Load Results

One of the primary reasons for choosing the control scheme shown in Fig. 16 was that operation at part load could be achieved with the reactor outlet temperature significantly reduced from the design value of 2300°F for 100% power. By operating at a lower temperature, the limitations imposed by creep are greatly reduced.

The part load characteristics for the vortex generator design and the low entrainment design may be compared from Tables 11 and 13. For the vortex generator design, a 10% step increase in load from steady state at 100% power will result in liquid (quality of about 80%) entering the turbine. For the 60% power case, a step increase of 10% will result in moisture at the turbine inlet for a reactor outlet temperature of 2093°F while for a reactor outlet temperature of 2123°F a 10% transient should cause no problems.

Table 13. Part Load Conditions for Low Liquid Entrainment Design (Boiler No. 9)

	Operation	Lithium Temperature at Reactor Exit (°F)	Potassium* Quality at Boiler Exit	Potassium Temperature at Boiler Exit (°F)
1.	Steady state at 100% power	2300	1.008	2144
2.	Step increase of 10% full power from steady state at 100% power	2300	0.942	2160.0
3.	Steady state at 60% power	2050	1.017	1968.4
4.	Step increase of 10% full power from steady state at 60% power	2050	0.964	1985

*Quality greater than 1.00 indicates superheat.

For the low liquid entrainment design, a 10% step increase in load from steady state at 100% power will also result in liquid (the vapor quality would be about 94%) entering the turbine. These results indicate that at full power the low entrainment design boiler can accept a larger step increase in power for a given allowable moisture content at the turbine inlet than the vortex generator design. However, at 60% load, the vortex design looks better for reactor outlet temperatures about 2125°F.

One disadvantage of the low liquid entrainment design is the possible damage due to thermal stresses created by mixing two liquid metal streams of different temperatures. Problems of this type have been experimentally investigated by Keyes and Krakoviak[24]. In the designs proposed here, the low temperature lithium flow from the parallel-flow region is mixed with the high temperature lithium flow from the counter-flow region. For the 100% and 60% power cases just described, the temperature differences are 140°F. These values may be too high for

reliable operation, hence it would probably be best to modify the design to reduce this temperature difference to less than 100°F for the entire normal operating range.

This problem may be reduced by considering a flow arrangement close to the one shown in Fig. 1 rather than one corresponding to that of Fig. 2. For this purpose, the dimensions for Boiler No. 8 were used with a lithium flow rate of 13.5 lb/sec in the parallel-flow region. (A 180° bend in the superheater region was also employed; the volume and weight for the resulting boiler will be approximately those values listed for Boiler No. 8 in Table 8). The results of these calculations are given in Table 14. The temperature difference between the flows being mixed is about 30° F or less for all steady state conditions listed, which appears acceptable. The part load response of this boiler appears to be better than that of either the vortex or the previous low entrainment designs.

Table 14. Part Load Conditions for Low Liquid Entrainment Design, Boiler No. 8 with Lithium Flow of 13.5 lb/sec in Parallel Flow Region, Plus a 180 deg Bend in the Superheater

	Operation	Lithium Temperature at Reactor Exit	Potassium* Quality at Boiler Exit	Potassium Temperature at Boiler Exit
		(°F)		(°F)
1.	Steady state at 100% power	2300	1.038	2220.1
2.	Step increase of 10% full power from steady state at 100% power	2300	1.036	2249.4
3.	Steady state at 60% power	2095	1.038	2020.3
4.	Step increase of 10% full power from steady state at 60% power	2095	1.033	2066.1

*Quality greater than 1.00 indicates superheat.

The above boilers were for the potassium system. For a comparison with the cesium system, the part load characteristics of Boiler No. 13 of Table 8 were calculated. The precepts for this analysis were, essentially, those listed in Table 12 for the potassium system. The correlation for the transition heat transfer coefficient developed by Peterson[23] for potassium was also used for cesium as a first estimate. A 180° bend in the dry-superheater region was assumed. The radial acceleration developed in the 180 deg bend was calculated assuming an average radius of curvature of 2.2 in. for the bundle. The heat transfer area in the boiler region, that in the bent portion of the dryer-superheater, and that in the straight portion of the dryer-superheater were 20, 35, and 18 ft^2, respectively. The results of these calculations are shown in Table 15. The indicated performance is similar to that listed in Table 14 for the potassium boiler.

Table 15. Part Load Conditions for Low Liquid Entrainment Design, Boiler No. 13 with Lithium Flow of 10.5 lb/sec in Parallel Flow Region, Plus a 180 deg Bend in The Superheater

	Operation	Lithium Temperature At Reactor Exit	Cesium* Quality at Boiler Exit	Cesium Temperature at Boiler Exit
1.	Steady state at 100% power	2300	1.008	2142
2.	Steady state at 60% power	2055	1.002	1896.7
3.	Step increase of 10% full power from steady state at 60% power	2055	1.018	2003.61

*Qualities greater than 1.00 indicate superheat.

While the above calculations indicate possible problems and solutions, additional experimentation and detailed calculations would be helpful to confirm the results.

The major conclusions are as follows:

1. The weight of the cesium boiler is greater than that for the potassium boiler by a factor of 1.3 for the vortex generator design and 2.4 for the low entrainment design.

2. The low entrainment design reduces the weight by a factor of about two relative to the vortex generator approach for potassium boiler-superheater units; for cesium, the savings in weight is only about 16%.

3. The volume for the low entrainment design is smaller than that for the vortex design by a factor of about 4.

REFERENCES

1. A. P. Fraas, D. W. Burton and L. V. Wilson, Design Comparison of Cesium and Potassium Vapor Turbine-Generator Units for Space Power Plants, ORNL-TM-2024 (Interagency Agreement 40-98-66, NASA Order W-12,353)(to be published).

2. H. C. Young and A. G. Grindell, Summary of Design and Test Experience with Cesium and Potassium Components and Systems for Space Power Plants, ORNL-TM-1833, (Interagency Agreement 40-98-66, NASA Order W-12,353)(to be published).

3. AiResearch Manufacturing Company of Arizona, Progress Report, SNAP 50/SPUR Contract AF 33 (615) - 2289, APS-5152-R3, July 1965.

4. J. A. Boppart, K. O. Parker and P. J. Berenson, Multiple-Tube Potassium Boiler Performance, AIAA Specialists Conference on Rankine Space Power Systems, CONF-651026, p. 327, October 1965.

5. J. R. Peterson, High-Performance Once-Through Boiling of Potassium in Single Tubes at Saturation Temperatures of 1500°F to 1750°F, NASA CR-842, August 1967.

6. J. A. Bond and G. L. Converse, Vaporization of High-Temperature Potassium in Forced Convection at Saturation Temperatures of 1800°F to 2100°F, NASA CR-843, July 1967.

7. A. H. Kreeger, J. N. Hodgson, and A. J. Sellers, Development of the SNAP-8 Boiler, AIAA Specialists Conference on Rankine Space Power Systems, CONF-651026, p. 285, October 1965.

8. K. M. Becker and G. Hernborg, Measurements of Burnout Conditions for Flow of Boiling Water in a Vertical Annulus, J. of Heat Transfer, ASME, p. 393 (1964).

9. G. F. Hewitt et al., Burn-Out and Nucleation in Climbing Film Flow, AERE-R 4374 (1963).

10. J. R. Peterson, High-Performance Once-Through Boiling of Potassium in Single Tubes at Saturation Temperatures of 1500°F to 1750°F, NASA CR-842, p. 87, August 1967.

11. Sze-Foo Chien and W. Ibele, Pressure Drop and Liquid Film Thickness of Two-Phase Annular and Annular-Mist Flows, J. of Heat Transfer, ASME Trans., pp. 89-96, February 1964.

12. L. S. Tong, Boiling Heat Transfer and Two-Phase Flow, John Wiley & Sons, p. 185 (1965).

13. N. A. Mozharov, An Investigation into the Critical Velocity at Which a Moisture Film Breaks Away from the Wall of a Steam Pipe, Teploenerg 6(2), 50-53, 1959, DSIR-Trans.-RTS-1581.

14. M. M. Yarosh, Boiling Studies for the Medium Power Reactor Experiment, pp. 88–104, AIAA Specialist Conference on Rankine Space Power Systems, Vol. II, USAEC Report TID-22508, October 1965.

15. J. R. Peterson, High-Performance Once-Through Boiling of Potassium in Single Tubes at Saturation Temperatures of 1500°F to 1750°F, p. 29, Fig. 9, NASA CR-842, August 1967.

16. A. P. Fraas and M. N. Ozisik, Heat Exchanger Design, John Wiley & Sons (1965).

17. J. R. Peterson, High-Performance Once-Through Boiling Potassium in Single Tubes at Saturation Temperatures of 1500°F to 1750°F, p. 80, Fig. 33, NASA CR-842, August 1967.

18. J. A. Bond and G. L. Converse, Vaporization of High-Temperature Potassium in Forced Convection at Saturation Temperatures of 1800°F to 2100°F, NASA CR-843, p. 178 (Fig. 56) and p. 134 (Table 3, Test Section No. 3).

19. A. P. Fraas, Medium-Power Reactor Experiment Quarterly Progress Report for Period Ending December 31, 1965, ORNL-3937.

20. A. P. Fraas, Flow Stability in Heat Transfer Matrices Under Boiling Conditions, USAEC Report ORNL-CF 59-11-1, Oak Ridge National Laboratory.

21. A. I. Krakoviak, Superheat Requirements with Boiling Liquid Metals, pp. 310-333 in Proceedings of 1963 High-Temperature Liquid-Metals Heat Transfer Technology Meeting, USAEC Report ORNL-3605, Oak Ridge National Laboratory, November 1964.

22. Space Power Plant Study, WANL-PR-(B)-009, NASA-CR-64507, December 1963.

23. J. R. Peterson, High-Performance Once-Through Boiling Potassium in Single Tubes at Saturation Temperatures of 1500°F to 1750°F, p. 51, August, 1967.

24. J. J. Keyes, Jr. and A. I. Krakoviak, High-Frequency Surface Thermal Fatigue Cycling of Inconel at 1405°F, Nuclear Science and Engineering, Vol 9, p. 462–474, 1961.

25. C. T. Ewing et al., High-Temperature Properties of Cesium, NRL Report 6246, U.S. Naval Research Laboratory, September 24, 1965.

26. C. T. Ewing et al., High-Temperature Properties of Potassium, NRL Report 6233, U.S. Naval Research Laboratory, September 24, 1965.

APPENDICES

Page Intentionally Left Blank

Appendix A

VORTEX GENERATOR DESIGN EQUATIONS

Equations for Boiler with Inserts

The following equations were used in the preliminary design calculations for the boilers with vortex generator inserts. These equations were taken from Ref. 5.

Equation A1: Heat transfer coefficient for superheated vapor.

$$\frac{h\,D_e}{k_g} = 0.359 \left[\frac{D_e\,V_H\,\rho_g}{\mu_g}\right]^{0.563} (N_{Pr_g})^{1/3}$$

where

- h = the heat transfer coefficient
- k_g = the thermal conductivity of the vapor
- μ_g = the viscosity of the vapor
- ρ_g = the density of the vapor
- N_{Pr_g} = the vapor Prandtl number

Also,

$$V_H = V_a\sqrt{1 + \left[\frac{\pi\,D_i}{P}\right]^2} \quad ,$$

where

- V_a = the velocity in the axial direction
- $\frac{D_i}{P}$ = the diameter to pitch ratio for the inserts

Equation A2: Radial acceleration

$$a_R = \frac{24}{D_i\, g}\left(\frac{XG}{\rho_g\sqrt{\frac{\rho_f}{\rho_g}}}\,\frac{\pi D_i}{P}\right)^2 ,$$

where

a_R = radial acceleration

D_i = tube ID

X = quality

ρ_f = density of the fluid

Equation A3: Pressure drop in superheater

$$\Delta P = -f_{e_g}\frac{\Delta Z}{D_e}\,\frac{G^2}{2\rho_g\, g}\left(\frac{L_H}{L}\right)^3 ,$$

where

ΔP = pressure drop

ΔZ = axial length

G = mass flow rate

g = 32.2

L = axial length

$$L_H = L\sqrt{1 + (\pi\,\frac{D_i}{P})^2}$$

$$f_{e_g} = 0.316/(N_{Re_g})^{1/4}$$

$$N_{Re_g} = \frac{D_e\, V_H\, \rho_g}{\mu_g}$$

μ_g = viscosity of the vapor

ρ_g = density of the vapor

Equation A4: Frictional pressure drop in two-phase flow

$$\Delta P = -f_{e_f} \frac{\Delta Z}{D_e} \frac{G^2}{2\rho_f g_c} \left(\frac{L_H}{L}\right)^3 \Phi ,$$

where

Φ = two-phase pressure drop multiplier (see Ref. 17)

$f_{e_f} = 0.316/N_{Re_f})^{1/4}$

$N_{Re_f} = \dfrac{D_e V_H \rho_f}{\mu_f}$

where μ_f is the viscosity of the liquid.

Equation A5:

$$D_e = \frac{D_i\left[1 + \left(\frac{D_{cb}}{D_i}\right)^2\right]}{1 + \frac{D_{cb}}{D_i} + \frac{1}{\pi}\left(1 - \frac{D_{cb}}{D_i}\right)} ,$$

where

D_{cb} = diameter of the central rod of the insert around which is the twisted ribbon.

Page Intentionally Left Blank

Appendix B

COMPUTER CODE FOR MINIMUM ENTRAINMENT DESIGN

The following describes a CEIR computer code used to calculate the boiler characteristics in the subcooled and boiling regions for the minimum entrainment approach. The code calculates the required heat transfer area and the tube length for both the subcooled and the boiling regions. The friction pressure drop across the boiling region is also calculated.

The code first calculates the requirements in the subcooled region and then those in the boiling region. The heat load in each region is divided by ten. The heat transfer area and the tube length required for each of these smaller sections is then calculated. This calculation consists of dividing the section heat load by the product of the overall heat transfer coefficient and the section LMTD.

The pressure drop in the boiling region is calculated assuming that annular flow exists over 100% of the boiling length. The calculation procedure is based on the work of Chien and Ibele (Ref. 11). First, the superficial Reynolds numbers are calculated:

$$Re'_g = 4\,\dot{m}_g/\pi D\,V_g$$

and

$$Re'_\ell = 4\,\dot{m}_\ell/\pi D\,V_\ell$$

Next, the two-phase friction factor is calculated by

$$f'_g = 3.680 \times 10^{-7}\, Re'^{0.582}_g\, Re'^{0.705}_\ell$$

Finally, the pressure drop is calculated by

$$\Delta P = -\, f'_g \frac{L}{D} \frac{\rho_g V'^2_g}{2g_c}$$

The following list is a step-by-step description of the code. The numbers listed correspond to the code statement number. The case illustrated is for a potassium boiler using tapered tubes; the design critical quality is 97%. A listing of the code appears at the end of this appendix.

4. L1 is a first guess for the total length of the subcooled and boiling regions.

5. N7 is the number of tubes.

9. D8 is the pressure drop over the boiling region and is initialized to zero.

10. L is the length from the boiler tube inlet.

11. Z7 is a control variable: if this has a value of 1, the quantities listed in statement 406 are not printed; any other value causes them to be printed.

15. A5 is the total heat transfer area and is initialized to zero.

16. V9 is the vapor viscosity in $lb_m/sec\text{-}ft$.

17. V8 is the liquid viscosity in $lb_m/sec\text{-}ft$.

18. R5 is the vapor density in lb_m/ft^3.

20. W1 is the primary fluid flow rate in the parallel flow region, lb/sec.

30. C1 is the specific heat of the primary fluid, $Btu/lb_m\text{-}°F$.

35. W4 is the flow rate of the working fluid, lb_m/sec.

40. K1 is the thermal conductivity of the primary fluid, $Btu/hr\text{-}ft\text{-}°F$.

50. C2 is the specific heat of the working fluid, $Btu/lb_m\text{-}°F$.

60. K2 is the thermal conductivity of the working fluid, $Btu/hr\text{-}ft\text{-}°F$.

65. X7 is the quality (fraction) at the exit of the boiling region.

71. W7 is the vapor flow rate, lb_m/sec, at the exit of the boiling region, and is found by multiplying the total flow rate by the quality at the exit.

80. B1 is the heat load, Btu/lb_m, in the subcooled region.

85. B2 is the heat of vaporization, Btu/lb_m.

90. B2 is multiplied by X7 to give the heat load in the boiling region.

100. T is a control variable used in statement 210, and is initialized to zero to indicate the subcooled region.

110. T1 is the inlet temperature of the primary fluid, °F.

120. T2 is the working fluid inlet temperature and is calculated by subtracting the heat load in the subcooled region divided by the specific heat from the temperature in the boiling region, °F.

130. R3 is the thermal resistance of the wall material which is 0.03 in. thick and has a thermal conductivity of 35 Btu/hr-ft-°F, hr-ft^2-°F/Btu.

150. This statement starts a loop, I = 1 to 20; for $1 \leq I \leq 10$, the counter I indicates the subcooled region; for $11 \leq I \leq 20$, the counter I indicates the boiling region. Each I designates a section of the boiler which transfers one-tenth the heat load for the region.

160. D2 is the tube ID which has an inlet value of 0.2 in. and an exit value of 0.45 in. for tapered tubes; for straight tubes D2 has a constant value of 0.45 in.

170. D1 is the tube OD, and is calculated by adding the wall thickness, 0.005 ft, to D2, ft.

175. S is the tube spacing, ft.

180. D5 is the hydraulic diameter on the shell side, ft.

185. A8 is the flow area on the shell side per unit cell, ft^2.

187. G1 is the flow rate on the shell side, lb/sec-ft^2.

190. H1 is the heat transfer coefficient on the shell side, Btu/hr-ft^2-°F.

$$h_1 = [7 + 0.025\ (GD)^{0.8}(C_p/k)^{0.8}]\frac{k}{D}$$

200. R1 is the thermal resistance on the shell side, hr-ft^2-°F/Btu.

210. This statement tests the control variable T; if $T > 0$ then control is transferred to statement number 270 indicating the boiling region; if $T \leq 0$, control is transferred to statement number 220 for the subcooled region.

220. H2 is the heat transfer coefficient of the working fluid in the subcooled region, Btu/hr-ft^2-°F.

$$h = [7 + 0.03\ (W/D)^{0.8}\ (C_p/k)^{0.8}]\ k/D$$

230. R2 is the thermal resistance on the tube side, hr-ft^2-°F/Btu.

240. T4 is the working fluid temperature after adding one-tenth the heat load of the subcooled region, °F. This is calculated by adding one-tenth the heat load of the subcooled region divided by the specific heat to the original fluid temperature.

250. H8 is the heat load, Btu/lb$_m$.

260. Q1 is the head load per section, Btu/hr; this is calculated by multiplying one-tenth the heat load in the subcooled region by the flow rate, W4, and by 3600 sec/hr.

265. This statement transfers control to statement number 310.

270. R2 is the thermal resistance on the tube side, hr-ft^2-°F/Btu.

271 to 278. These statements cause the calculation of constants used in the pressure drop calculation in the boiling region.

280. T4 is the temperature in the boiling region.

281. M1 is the vapor flow rate in the boiling region, lb$_m$/sec.

282. M2 is the liquid flow rate in the boiling region, lb$_m$/sec.

283. S7 is the superficial vapor Reynolds number; this is calculated as four times the vapor flow rate (lb$_m$/sec) divided by the product of π, the hydraulic diameter (ft) and the vapor viscosity (lb$_m$/sec-ft).

284. S8 is the superficial liquid Reynolds number; this is calculated as four times the liquid flow rate (lb$_m$/sec) divided by the product of π, the hydraulic diameter (ft) and the liquid viscosity (lb$_m$/sec-ft).

285. F is the superficial friction factor of the two-phase flow:

$$F = 3.68 \times 10^{-7}\ (S7)^{0.582}\ (S8)^{0.705}\ .$$

286. V1 is the vapor velocity, ft/sec; this is calculated as

$$M1/(\frac{\pi D^2}{4}\ \rho_g)\ .$$

290. H8 is the heat load in the boiling region, Btu/lb_m.

300. Q1 is the heat load per section, Btu/hr; this is calculated by multiplying one-tenth the heat load in the subcooled region by the flow rate, W4, and by 3600 sec/hr.

310. T3 is the primary fluid temperature after giving up one-tenth the region heat load, °F.

320. U is the overall heat transfer coefficient, $Btu/hr\text{-}ft^2\text{-}°F$.

330. O1 is the temperature difference between the working fluid and the primary fluid at the inlet of the section.

340. O2 is the temperature difference between the working fluid and the primary fluid at the exit of the section.

345. This statement transfers control to 352 if O1/O2 is greater than 1.5.

346. This statement transfers control to 352 if O1/O2 is less than 0.66.

350. L9 is the section MTD, and is calculated as the average value of O1 and O2.

351. This statement transfers control to 360.

352. L9 is the section LMTD and is calculated as

$$L9 = (O1 - O2)/\ln\left(\frac{O1}{O2}\right) .$$

360. A1 is the mean heat transfer area per foot of tube for one tube, (ft^2/ft).

361. A1 is multiplied by the number of tubes to give the mean heat transfer area per foot of tube for the boiler, (ft^2/ft).

365. A9 is the heat transfer area required for the section, ft^2; This is calculated as the heat load divided by the overall heat transfer coefficient and the LMTD.

370. A5 is the sum of the required heat transfer area.

375. L8 is the tube length required for this section, ft; this is calculated as the area required divided by the available area per foot of boiler.

380. L is the sum of the required tube length, ft.

381. This statement transfers control to 390 if I indicates the subcooled region.

382. D9 is the two-phase pressure drop over the section, psi; this is calculated as

$$D9 = F \frac{\rho}{2g} \frac{L}{D} \frac{V^2}{144} .$$

383. D8 is the sum of the pressure drop in the boiling region, psi.

390. T1 is assigned the value of T3; this establishes the primary fluid temperature at the inlet to the next section.

400. T2 is assigned the value of T4; this establishes the working fluid temperature at the inlet to the next section.

401. This statement transfers control to 404 unless I = 20.

402. Q is the heat flux at the exit of the boiling region as calculated by the product of the overall heat transfer coefficient and the temperature difference between the fluids.

403. This statement prints the heat flux, the overall heat transfer coefficient, and the temperature difference between the fluids for the conditions at the exit of the boiling region.

404. This statement transfers control to 410 if Z7 = 1.

405. This statement calculates Q (see 402).

406. This statement prints the total length up to the section length, the section heat transfer area, the overall heat transfer coefficient, and the heat flux at the exit of the section.

410. This statement transfers control to 430 if I = 10.

420. This statement transfers control to 440.

430. T is assigned the value of one to indicate the boiling region.

431. The length and heat transfer area for the subcooled region are printed.

440. This statement indicates the end of the loop, I is increased by one and control is returned to statement 160 if $I \leq 20$.

450. The length required in the subcooled and boiling region is printed.

451. The area required in the subcooled and boiling region is printed.

455. The pressure drop is printed.

460. This statement assigns the calculated length to the assumed length, Ll.

470. This statement transfers control to 5. If the assumed length is sufficiently close to the calculated length, the calculations are manually terminated.

52308. This statement signifies the end of the program.

```
4 LET L1=5
5 LET N7=58
9 LET D8=0
10 LET L=0
11 LET Z7=1
15 LET A5=0
16 LET V9=1.545E-5
17 LET V8=8.05E-5
18 LET R5=1/2.7287
20 LET W1=9.6
30 LET C1=.9815
35 LET W4=2.22
40 LET K1=29.54
50 LET C2=.21
60 LET K2=13.6
65 LET X7=.97
70 LET W2=.03865
71 LET W7=X7*W2
80 LET B1=26.52
85 LET B2=718.55
90 LET B2=X7*B2
100 LET T=0
110 LET T1=2300
120 LET T2=2125-B1/C2
130 LET R3=.03/(35*12)
150 FOR I=1 TO 20
160 LET D2=(.2+.25*L/L1)/12
170 LET D1=D2+.005
175 LET S=.0625/12
180 LET D5=(D1*(((D1+S)/D1)↑2*1.102-1))
185 LET A8=.433*(D1+S)↑2-D1↑2*.39
187 LET G1=W1*3600/(2*N7*A8)
190 LET H1=(7+.025*(G1*D5)↑.8*(C1/K1)↑.8)*K1/D5
200 LET R1=1/H1
210 IF T>0 THEN 270
220 LET H2=(7+.03*(W2/D2)↑.8*(C2/K2)↑.8)*K2/D2
230 LET R2=1/H2
240 LET T4=T2+B1/2.1
250 LET H8=B1
260 LET Q1=B1*W4*360
265 GO TO 310
270 LET R2=1.E-4
271 LET Y1=3.14159*D2
272 LET Y2=Y1*V9
273 LET Y3=4/Y2
274 LET Y4=Y1*V8
275 LET Y5=4/Y4
276 LET Y6=288*32.174*D2
277 LET Y7=R5/Y6
278 LET Y8=3.14159*D2↑2*R5/4
```

```
280 LET T4=2125
281 LET M1=W7/20+(I-11)*W7/10
282 LET M2=W2-M1
283 LET S7 =Y3*M1
284 LET S8=Y5*M2
285 LET F=3.68E-7*S7↑.582*S8↑.705
286 LET V1=M1/Y8
290 LET H8=B2
300 LET Q1=B2*W4*360
310 LET T3=T1-H8*W4/(W1*C1*10)
320 LET U=1/(R1+R2+R3)
330 LET O1=T1-T2
340 LET O2=T3-T4
345 IF (O1/O2)>1.5 THEN 352
346 IF (O1/O2)<.66 THEN 352
350 LET L9=(O1+O2)/2
351 GO TO 360
352 LET L9=(O1-O2)/LOG(O1/O2)
360 LET A1=3.14159*(D2+.03/12)
361 LET A1=A1*N7
365 LET A9=Q1/(U*L9)
370 LET A5=A5+A9
375 LET L8=A9/A1
380 LET L=L+L8
381 IF I<11 THEN 390
382 LET D9=(F*Y7*V1↑2)*L8
383 LET D8=D8+D9
390 LET T1=T3
400 LET T2=T4
401 IF I<20 THEN 404
402 LET Q=U*O2
403 PRINT "Q,U,DT AT EXIT ARW",Q,U,O2
404 IF Z7=1 THEN 410
405 LET Q=U*O2
406 PRINT L,L8,A9,U,Q
410 IF I=10 THEN 430
420 GO TO 440
430 LET T=1
431 PRINT "FOR SUBCOOL L AND A ARE",L,A5
440 NEXT I
450 PRINT "L",L
451 PRINT "A",A5
455 PRINT "DP",D8
460 LET L1=L
470 GO TO 5
52308 END
```

Page Intentionally Left Blank

Appendix C

COMPUTER CODES FOR PART LOAD ANALYSIS

Low Entrainment Approach

```
10 READ T8,H1,L1,C1
12 DATA 2125,719,1.0,.29
20 LET T9=T8
25 LET T=2295
30 LET T1=T
35 LET W1=9.3
40 LET W2=17-W1
45 LET U=4700
50 LET W9=L1*2.22
150 LET T2=T1-T9
160 LET Z1=0
170 LET A9=0
180 LET Q9=0
200 FOR I=1 TO 191
210 GOSUB 900
220 LET T1=T1-Q2/(W1*.9815*3600)
230 LET T2=T1-T9
270 IF Z1=1 THEN 320
275 IF X1<.3 THEN 370
280 LET Q5=850000*(1-X1)
290 IF Q1<Q5 THEN 370
300 PRINT "BO AT",I,"LI T",T1,"QUAL",X1,"Q/A",Q1
310 LET Z1=1
320 LET D=2*SQR(.15*I/(3.142*58*3.7)+.01)
330 LET G=W9*4/(3.142*D↑2)
331 LET G=G*144/58
340 LET H5=.6*28*(G/10)↑.8/D↑.2
350 GOSUB 1000
360 LET U=1/(1/H6+1.13E-4)
370 NEXT I
390 LET T3=T1
400 PRINT "AT BOIL EXIT LI T AND X ARE",T1,X1
402 LET Q7=Q9
405 LET N=27
406 LET Z=1
408 LET T=2278
410 FOR I=1 TO N
415 LET A9=4.25*W9↑2*X1↑2*Z
420 LET T2=T-T9
430 LET H5=.6*28*(L1*4.26)↑.8/.124↑.2
440 IF X1>=1 THEN 480
```

```
450 GOSUB 1000
451 IF Z=0 THEN 460
452 LET U=3*(H6+H5)/2
460 LET U=3*H6
470 GO TO 490
480 LET U=3*H5
490 GOSUB 900
495 LET T=T+Q2/(W2*.9815*3600)
540 IF X1<=1 THEN 570
560 LET T9=T9+Q2/(3600*W9*C1)
570 NEXT I
580 IF N>28 THEN 650
600 PRINT "AT BEND EXIT K T AND X ARE",T9,X1
610 LET Z=0
620 LET N=51
625 LET Z8=0
630 GO TO 410
650 PRINT "AT EXIT K T AND X ARE",T9,X1
660 LET Q6=Q9-Q7
665 PRINT "EX LI TEM",T
670 LET T5=T-Q6/(W2*.9815*3600)
680 LET T4=((W1*T3)+(W2*T5))/17
690 PRINT "T P",T3,"T C",T5,"T M",T4
890 GO TO 1200
900 LETQ1=U*T2
910 LET Q2=.1*Q1
920 LET Q9=Q9+Q2
930 LET Q8=Q9/(3600*W9)
940 LET X1=Q8/H1
950 RETURN
960 GO TO 1200
1000 LET Z2=(1+A9)↑.2*2.55E5
1005 LET N5=T2
1007 IF N5>30 THEN 1012
1009 LET N5=30
1012 LET X3=X1
1013 IF X3<1 THEN 1016
1014 LET Z4=0
1015 GO TO 1020
1016 LET Z3=(1/X3-1)↑.7/N5↑2
1017 LET Z4=Z3*Z2
1018 IF Z4>0 THEN 1020
1019 LET Z4=0
1020 LET H6=H5*(1+Z4)
1030 RETURN
1200 END
```

```
10 READ T8,H1,L1,R3
12 DATA 2125,719,1.0,.29
15 LET C1=.3
20 LET T9=T8
25 LET T=2203.5
30 LET T1=T
35 LET W1=17
40 LET W2=17-W1
45 LET U=1650
50 LET W9=L1*2.22
150 LET T2=T1-T9
160 LET Z1=0
170 LET A9=0
180 LET Q9=0
200 FOR I=1 TO 68
210 GOSUB 900
220 LET T1=T1+Q2/(W1*.9815*3600)
230 LET T2=T1-T9
270 IF Z1=1 THEN 320
275 IF X1<.3 THEN 370
280 LET Q5=850000*(1-X1)
290 IF Q1<Q5 THEN 370
300 PRINT "BO AT",I,"LI T",T1,"QUAL",X1,"Q/A",Q1
310 LET Z1=1
320 LET D=.494
330 LET G=W9/.056
340 LET H5 =.2145*(6600*G)↑.563
345 LET A9=(X1*G*R3*3.142)↑2
350 GOSUB 1000
360 LET U=1/(1/H6+5.064E-4)
361 IF X1<1 THEN 370
362 LET T9=T9+Q2/(3600*W9*C1)
370 NEXT I
400 PRINT "AT BOIL EXIT LI T AND X ARE",T1,X1
401 PRINT "K T IS",T9
890 GO TO 1200
900 LETQ1=U*T2
```

```
910 LET Q2=.5*Q1
920 LET Q9=Q9+Q2
930 LET Q8=Q9/(3600*W9)
940 LET X1=Q8/H1
950 RETURN
960 GO TO 1200
1000 LET Z2=(1+A9)↑.2*2.55E5
1005 LET N5=T2
1007 IF N5>30 THEN 1012
1009 LET N5=30
1012 LET X3=X1
1013 IF X3<1 THEN 1016
1014 LET Z4=0
1015 GO TO 1020
1016 LET Z3=(1/X3-1)↑.7/N5↑2
1017 LET Z4=Z3*Z2
1018 IF Z4>0 THEN 1020
1019 LET Z4=0
1020 LET H6=H5*(1+Z4)
1030 RETURN
1200 END
```

INTERNAL DISTRIBUTION

1. S. E. Beall
2. D. L. Clark
3. W. B. Cottrell
4. F. L. Culler
5. J. H. DeVan
6. J. R. DiStefano
7. B. Fleischer
8–27. A. P. Fraas
28. A. G. Grindell
29. W. O. Harms
30. P. N. Haubenreich
31. H. W. Hoffman
32. R. S. Holcomb
33. W. R. Huntley
34. D. H. Jansen
35. P. R. Kasten
36. R. L. Klueh
37. M. E. Lackey
38. J. A. Lane
39. W. J. Larkin, AEC-ORO
40. M. E. LaVerne
41. A. P. Litman
42. M. I. Lundin
43. R. N. Lyon
44. R. E. MacPherson
45. H. C. McCurdy
46. A. J. Miller
47. A. M. Perry
48. T. T. Robin
49. M. W. Rosenthal
50. G. Samuels
51. A. Savolainen
52. M. J. Skinner
53. I. Spiewak
54. D. A. Sundberg
55. D. B. Trauger
56. A. M. Weinberg
57. G. D. Whitman
58. L. V. Wilson
59. H. C. Young
60. ORNL Patent Office
61–62. Central Research Library (CRL)
63–64. Y-12 Document Reference Section (DRS)
65–84. Laboratory Records (LRD)
85. Laboratory Records - Record Copy (LRD-RC)

EXTERNAL DISTRIBUTION

86. J. J. Lynch, RNP, NASA, Washington, D.C.
87–96. S. V. Manson, RNP, NASA, Washington, D.C.
97. F. Schulman, RNP, NASA, Washington, D.C.
98. W. H. Woodward, RN/D, NASA, Washington, D.C.
99. R. L. Cummings, SPSD, NASA-LRC, Cleveland, Ohio
100. R. E. English, SPSD, NASA-LRC, Cleveland, Ohio
101. J. A. Heller, SPSD, NASA-LRC, Cleveland, Ohio
102. B. Lubarsky, SPSD, NASA-LRC, Cleveland, Ohio
103. T. P. Moffitt, FSCD, NASA-LRC, Cleveland, Ohio
104. T. A. Moss, SPSD, NASA-LRC, Cleveland, Ohio
105. L. Rosenblum, M&SD, NASA-LRC, Cleveland, Ohio
106. W. L. Stewart, FSCD, NASA-LRC, Cleveland, Ohio
107. R. N. Weltmann, SPSD, NASA-LRC, Cleveland, Ohio
108. N. Grossman, DRD&T, AEC, Washington, D.C.
109. C. Johnson, SNS, AEC, Washington, D.C.
110. G. Leighton, SNS, AEC, Washington, D.C.
111. O. E. Dwyer, Brookhaven National Laboratory, Upton, N.Y.
112. D. H. Gurinsky, Brookhaven National Laboratory, Upton, N.Y.
113. J. Hadley, Lawrence Radiation Laboratory, Livermore, California
114. D. R. Bartz, Jet Propulsion Laboratory, Pasadena, California
115. J. Davis, Jet Propulsion Laboratory, Pasadena, California

116. D. Elliot, Jet Propulsion Laboratory, Pasadena, California
117. L. Hays, Jet Propulsion Laboratory, Pasadena, California
118–121. M. A. Zipkin, General Electric Company, Cincinnati, Ohio
122–123. R. D. Gruntz, AiResearch, Phoenix, Arizona
124–125. W. D. Puchot, Astronuclear Lab., Westinghouse Electric, Pittsburgh, Pennsylvania
126–127. V. R. Degner, Rocketdyne Division, N.A.A., Canoga Park, California
128–129. R. Gordon, SNAP-8 Division, Aerojet-General, Azusa, California
130. R. H. Chesworth, Aerojet-General Nucleonics, San Ramon, California
131. J. Edward Taylor, TRW, Inc., Cleveland, Ohio
132. C. L. Walker, Allison Division of General Motors, Indianapolis, Indiana
133. B. Sternlicht, Mechanical Technology Incorporated, Latham, N.Y.
134. R. Myers, Pratt and Whitney Aircraft Corporation, E. Hartford, Conn.
135. S. Greenberg, Argonne National Laboratory, Argonne, Illinois
136. R. L. Eichelberger, Atomics International, Canoga Park, California
137. K. Goldmann, United Nuclear Corporation, White Plains, New York
138–152. Division of Technical Information Extension (DTIE)
153. Laboratory and University Division (ORO)